



High-rise timber buildings against wind-induced vibration: A comprehensive study on design criteria, design codes and design cases

Haoze Chen ^a, Libo Yan ^{a,b,*}, Junaid Ajaz Dand ^a

^a Department of Organic and Wood-Based Construction Materials, Institute for Building Materials, Concrete Construction and Fire Safety, Technische Universität Braunschweig, Hopfgarten 20, Braunschweig, 38102, Germany

^b Fraunhofer Institute for Wood Research Wilhelm-Klauditz-Institut WKI, Riedenkamp 3, Braunschweig, 38108, Germany

ARTICLE INFO

Keywords:

Timber building
High-rise building
Wind-induced vibration
Serviceability
Design codes
Design cases

ABSTRACT

Timber construction offers significant environmental advantages, and the recent rise of timber buildings, culminating in record-setting high-rises, demonstrates a growing trend toward tall timber structures. However, the low self-weight of timber material makes high-rise timber buildings particularly vulnerable to wind-induced vibrations, which often governs design. Compounding this challenge, the principal design codes and criteria do not offer comprehensive, specific provisions for combined wind-vibration effects from the perspective of timber building. This study aims to 1) evaluate design of timber buildings against wind-induced vibration to provide practical guidance, 2) catalogs current serviceability criteria (i.e. ISO 10137, ISO 6897, AIJ-Guidelines, NBCC-Guidelines, ASCE 7–22, AS/NZS 1170.0 and 1170.2, Eurocode 5) for wind-generated accelerations and displacements of buildings, 3) identify gaps of wind-induced vibration design methods outlined in leading international codes (i.e. Eurocode 1–4, ASCE 7–22, AIJ-RBL, NBCC, AS/NZS 1170.2) from regions actively engaged in timber construction, and 4) analyze the wind-design strategies employed in five completed high-rise timber building projects. Results show that current code methods are constrained by simplified assumptions with strict requirement on building dimensions and profile, lacking timber-specific parameters, e.g. damping and natural frequency. Existing codes do not yet provide sufficiently comprehensive methods for evaluating combined vibration effects, and most realized projects have only partially considered the serviceability requirements, which, although, are not mandatory in current design practice. By integrating these criteria, highlighting the limitations of existing codes, and drawing lessons from existing tall timber structures, this study offers clear guidance for engineers seeking to evaluate and mitigate wind-induced vibrations of timber buildings, thereby supporting the reliable design of future high-rise timber buildings.

List of symbols

$A_{\theta}(t)$	Peak rotational angular velocity
$\bar{\alpha}$	Mean hourly wind-speed power law exponent
a_{cri}	Acceleration evaluation criterion
a_e	Equivalent translational acceleration for evaluation of torsional acceleration
$a_{(x,y,z)}$	Overall peak acceleration
B	Background turbulence factor
b	Building width (horizontal dimension of a building measured normal to the wind direction)
b_{eff}	Effective width of windward face of the building
C_{eh}	Exposure factor
C_{lat}	Lateral force coefficient

(continued on next column)

(continued)

List of symbols

$C_{lat,0}$	Basic value of lateral force coefficient
$C_{f,t}$	Torsional moment coefficient
$C_{f,x}$	Wind force coefficient (along-wind)
$C_{f,y}$	Across-wind overturning moment coefficient
$C_{fig,windward}$	External aerodynamic shape factor on the windward surface
$C_{fig,leeward}$	External aerodynamic shape factor on the leeward surface
C_{pe1}	External pressure coefficients on the windward face
C_{pe2}	External pressure coefficients on the leeward face
D	Along-wind effects
d_{eff}	Effective depth of the building
E	Modulus of elasticity of a material

(continued on next page)

* Corresponding author. Department of Organic and Wood-Based Construction Materials, Institute for Building Materials, Concrete Construction and Fire Safety, Technische Universität Braunschweig, Hopfgarten 20, 38102, Braunschweig, Germany.

E-mail addresses: l.yan@tu-braunschweig.de, libo.yan@wki.fraunhofer.de (L. Yan).

<https://doi.org/10.1016/j.dibe.2025.100815>

Received 1 September 2025; Received in revised form 6 November 2025; Accepted 22 November 2025

Available online 2 December 2025

2666-1659/© 2025 The Authors. Published by Elsevier Ltd. This is an open access article under the CC BY license (<http://creativecommons.org/licenses/by/4.0/>).

(continued)

List of symbols	
F	Gust energy ratio
F_i	Associated wind force on floor i
$F_{res,x}$	Resonant along-wind forces
f_n	Vibration frequency
G	Gust-effect factor
G_D	Along-wind gust effect factor
g_r	Peak factor
H	Building height in foot
h	Building height in meter
h_{ave}	Average height of the building roof above ground
I_b	Moment of inertia of the cross-section
I_u	Turbulence intensity at the height where it has the largest movement
I_z	Intensity of turbulence at the reference height \bar{z}
K	Mode shape correction factor (along-wind)
K_a	Area reduction factor
$K_{c,e}$	Combination factor
K_l	Local pressure factor
K_p	Porous cladding reduction factor
$K_{p,ac}$	Peak factor for across-wind displacement
K_s	Size reduction function
K_t	Mode shape correction factor (torsional)
K_y	Mode shape correction factor (across-wind)
$K_{y,dis}$	Mode shape factor for across-wind displacement
K_w	Effective correlation length factor
k	Terrain factor
L	Across-wind effects
L_j	Correlation length for across-wind effect
L_z	Integral length scale of turbulence at the reference height \bar{z}
$M_{ac,max}$	Maximal across-wind resonant component of base overturning moment
\bar{M}_{al}	Deviation of resonant along-wind base moment
M_s	Equivalent mass
$M_{t,max}$	Maximum resonant torsional moment
$m_{1,t}$	Generalized mass for torsional vibration
$m_{1,x}$	Generalized mass for along-wind vibration
$m_{1,y}$	Generalized mass for across-wind vibration
m_c	Concentrated mass of a structure for dynamic calculation
n	Lowest natural frequency of the building
n_1	Natural frequency of the first mode in calculated wind direction
$n_{1,t}$	Natural frequency of the first mode in torsional direction
$n_{1,x}$	Natural frequency of the first mode in along-wind direction
$n_{1,y}$	Natural frequency of the first mode in across-wind direction
R	Resonant response factor
$R_{eff,t}$	Effective resonant factor for torsional effect
$R_{eff,x}$	Effective resonant response factor for along-wind response (Rewritten from the original resonant response factor R in codes/standards due to the standardization of the formula)
$R_{eff,y}$	Effective resonance factor for across-wind effect
r	Distance from the rotational center to the evaluation point of a structure
r_{max}	Distance from the furthest point away from the center of rigidity at the top of the building
s	Size reduction factor
S_c	Scruton number
S_t	Strouhal number
T	Averaging time of wind duration
T_t	Torsional effects
V_{10}	Hourly mean wind speeds for 10-years return period
$V_{10-min,1}$	10-min mean wind speed in a one-year return period
V_{50}	Hourly mean wind speeds for 50-years return period
\bar{V}	Mean wind velocity
V_{crit}	Critical wind velocity
$V_{m,L}$	Mean wind velocity in the central of correlation length
V_n	Reduced velocity
V_T	Normalized velocity for torsional acceleration calculation
\bar{V}_z	Mean wind velocity at the reference height \bar{z}
v	Up-crossing rate
\hat{x}_{max}	Maximum along-wind displacement
x_i	Floor horizontal deflection
$\bar{x}(z)$	Standard deviation of acceleration in x-axial (along-wind) direction at the point with the height of z
$\hat{x}(z)_{max}$	Wind-induced peak acceleration in the along-wind direction at height z
\hat{y}_{max}	Maximal across-wind displacement
\hat{y}_{max}	Maximal across-wind acceleration
z	Height of the evaluation point of a structure
\bar{z}	Reference height

(continued on next column)

(continued)

List of symbols	
\hat{z}	Peak acceleration components about z-axis (torsional direction)
β_t	Damping ratio in torsional direction
β_x	Damping ratio in along-wind direction
β_y	Damping ratio in across-wind direction
$\hat{\theta}_{max}$	Peak rotational velocity (angular)
$\hat{\theta}_{max}$	Peak torsional acceleration
$\phi_{1,t}(z)$	Fundamental mode shape in the z-axial (torsional) direction evaluated at height z
$\phi_{1,x}(z)$	Fundamental mode shape in the x-axial (along-wind) direction evaluated at height z
$\phi_{1,y}(z)$	Fundamental mode shape in the y-axial (across-wind) direction evaluated at height z
ϕ_{max}	Mode shape value at the point with maximum amplitude
$\mu(z)$	Mass per unit height
ρ	Air density
ρ_B	Density of the building
ρ_c	Relationship between the peak acceleration of the largest component and that of the second-largest component
ξ	Mode shape exponential coefficient
Δ_{max}	Maximum along-wind lateral deflection at the top of the building
δ	Logarithmic decrement of damping
$\delta_{t,s}$	Logarithmic decrement of structural damping in torsional direction
δ_x	Logarithmic decrement of total damping in along-wind direction
$\delta_{x,s}$	Logarithmic decrement of structural damping in along-wind direction
$\delta_{x,a}$	Logarithmic decrement of aerodynamic damping for the fundamental mode in along-wind direction
$\delta_{x,d}$	Logarithmic decrement of damping due to special devices in along-wind direction
δ_y	Logarithmic decrement of total damping in across-wind direction
$\delta_{y,s}$	Logarithmic decrement of structural damping in across-wind direction
$\delta_{y,a}$	Logarithmic decrement of aerodynamic damping for the fundamental mode in across-wind direction
$\delta_{y,d}$	Logarithmic decrement of damping due to special devices in across-wind direction
γ_{LT}	Combination factor

1. Introduction

Achieving the Paris Agreement targets (agreement, 2017) and the carbon-neutrality goals embodied in initiatives such as the European Green Deal (Gheuens et al., 2024) requires continuous emission reduction. The building sector accounts for about 39% of global greenhouse-gas emissions (World Green Building Council, 2019), of which construction materials alone contribute roughly 11% (World Green Building Council, 2019). Substituting these carbon-intensive materials with low-emission alternatives is therefore essential. Timber is one of the oldest and widely available building materials, offering clear environmental advantages. Life-cycle assessments consistently show that mass-timber buildings generate, on average, about 40% less greenhouse-gas emissions than comparable reinforced-concrete or steel structures (Duan et al., 2022). In addition, structural timber sequesters carbon for decades, roughly the time required for new trees to mature, helping to balance the carbon cycle (Porteron, 2023). These attributes make timber a sustainable and environmentally friendly choice for construction.

Reflecting these benefits, the number timber buildings has risen sharply over the past two decades (Yan et al., 2025; Svatoš-Ražnjević et al., 2022). Amid rapid urbanization, high-rise construction offers a practical solution for housing growing populations. As a result, there has been a rise in high-rise timber buildings, such as Mjøstårnet in Norway (Liven and Abrahamsen, 2023) (85.4 m (Council on Tall Buildings and Urban Habitat, 2022; Abrahamsen, 2017)) and Ascent in the USA (Fernandez et al., 2020) (86.6 m (Council on Tall Buildings and Urban Habitat, 2022)), both of which continue to set height record. Given their substantially lower climate impact compared to reinforced-concrete or steel high-rise buildings (Yan et al., 2025; Skullestad et al., 2016), it is expected that high-rise timber structures will not only become more common but also achieve even greater heights in the coming years.

Designing high-rise timber structures presents several technical challenges. Key challenges include fire safety, connection detailing, acoustic performance, and moisture sensitivity etc. Notably, timber material's lower self-weight compared to reinforced concrete and steel increases its susceptibility to wind-induced vibrations. Three principal vibration components could influence the performance of the building as illustrated in Fig. 1, i.e., along-wind vibration, across-wind vibration and torsional vibration. These wind-induced vibrations can act individually or in combination, causing accelerations and displacements that often control serviceability and can govern the overall structural design of high-rise timber buildings in real design practices (Fernandez et al., 2020; Laurent et al., 2023).

In current practice, the design of high-rise timber buildings to mitigate wind-induced vibrations is often incomplete. While along-wind effects are usually considered, such as in the case of the Mjøstårnet in Norway (Abrahamsen, 2017), across-wind, torsional, and especially combined responses are frequently neglected (please see section 4). Meanwhile, many national codes do not provide calculation methods for all three vibration components or their combined effects (e.g., the Eurocode 1–4 (Eurocode 1-4, 2010)). This implies that structural designers may need to reference multiple standards/codes, or even those beyond their local jurisdiction, to comprehensively account for wind-induced vibrations in all directions. Consequently, there is a clear need for an integrated review and summary of code-based design criteria and methods for wind-induced vibration in timber structures, specifically from the perspective of timber structural engineers.

Previous studies have not sufficiently addressed these technical challenges. To date, no comprehensive review/study has examined the wind-induced vibration design of high-rise timber structures. Although Aloisio et al. (2023) discussed vibration issues in timber structures, their focus was primarily on acoustic problems in floors, with only brief mention of wind-induced effects, providing limited guidance for practitioners in wind design. Similarly, Kwon and Kareem (Kwon and Kareem, 2013) reviewed wind-effect design standards but concentrated solely on calculation methods, without summarizing the design criteria for wind-induced vibration. Their work also lacked detailed discussion on maximum wind-induced displacement calculations, the applicability limits of vibration formulas, and the combined evaluation of multi-directional wind effects. Most critically, the discussion of standard-based vibration calculations was not approached from a timber structural designer's viewpoint, overlooking key challenges for design of tall timber structures, e.g. selection of damping value and natural frequency. In addition, completed high-rise timber projects offer valuable empirical insights that should be systematically summarized to inform future wind-resistant design. This study is therefore developed in

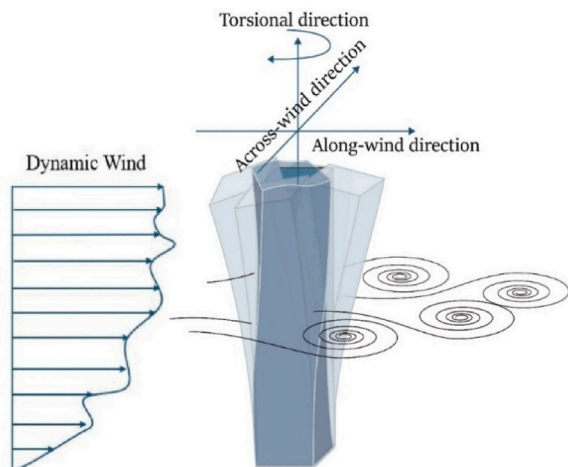


Fig. 1. Schematic of wind-induced vibration effects on buildings.

response to both the growing trend of high-rise timber construction and the evident research gap in wind-induced vibration design highlighted above.

This study focuses on the design of high-rise timber structures concerning wind-induced vibrations. The current serviceability criteria for wind-induced accelerations and displacements are catalogued, followed by examinations on the wind-vibration provisions in the principal international codes (i.e. Eurocode 1–4, ASCE 7–22, AIJ-RBL, NBCC, AS/NZS 1170.2) used in regions with substantial timber-building activity, highlighting their applicability and limitations for timber building design. Finally, this study analyzes existing high-rise timber buildings from a wind engineering perspective. The goal is to provide structural engineers with practical guidance for evaluating along-wind, across-wind, torsional, and combined wind effects, thereby enabling the reliable design of future high-rise timber buildings. At the same time, the study identifies gaps and limitations among existing criteria, codes, and realized projects, offering a basis for future code development and further research of high-rise timber buildings.

In this context, the following three core research questions are explored throughout the study:

- (1) Are the serviceability criteria, computational procedures prescribed by codes, and actual design practices in completed timber projects consistently aligned, or do gaps exist between them? For instance, do the criteria specify performance requirements, such as combined acceleration limits, that are not directly assessable through the available code methods or are sometimes neglected in real projects?
- (2) What are the main limitations of current international design codes in addressing wind-induced vibrations for high-rise timber structures?
- (3) What experiences and insights can be drawn from existing high-rise timber projects to inform future wind-vibration design and code development?

2. Design criteria

Building design is typically based on the Limit State Design (LSD) approach, which requires compliance with two principal criteria: the ultimate limit state (ULS) criteria and the serviceability limit state (SLS) criteria. This paper focuses on wind-induced vibration issues of timber buildings. Under ULS, wind loads are generally treated as static and combined with vertical loads, which do not sufficiently address vibration responses and therefore fall outside the main scope of this discussion. Accordingly, this section briefly introduces ULS wind design criteria, while placing emphasis on the SLS criteria related to wind actions.

2.1. Ultimate limit state (ULS) criteria

ULS criteria ensure structural safety and stability under extreme events. Normally, wind loads will be combined with permanent (dead), imposed (live), and other environmental loads, each with their prescribed load factors, to verify that no member or connection exceeds its design capacity. Numerous load combinations exist, and they do not directly address wind-induced vibration; therefore, detailed discussion is omitted. Instead, the following points highlight potential ULS issues arising from wind loads or wind-induced vibration.:

- **Strength and Overall Stability:** Structures must resist factored wind loads, along with other combined loads, without overstressing or failing any component or connection.
- **Overturning Resistance:** The total overturning moment caused by wind must be balanced by the restoring moment from gravity loads. A minimum overturning-safety factor of about 1.5 is commonly recommended (IBC, 2024), especially critical for lightweight timber

high-rise buildings, where the lower self-weight of timber materials provides less stabilizing moment compared to buildings made of reinforced concrete or steel.

- Second-Order (P-Δ) Effects: Wind-induced deflection introduces additional moments as gravity loads act on the displaced structure. For very flexible or slender buildings, P-Δ effects can considerably reduce effective lateral and vertical stiffness. Therefore, designers limit lateral drift and include second-order analysis in ULS checks to prevent destabilizing feedback.

2.2. Serviceability limit state (SLS) criteria

In building design, particularly regarding wind loads, it is crucial to ensure not only the structural capacity under but also to set limits on vibrations to maintain the building’s functional and operational performance. These limits are defined by SLS criteria. Due to acceleration from vibrations, occupants may feel the building shake or notice visible misalignments, such as shifting edges of adjacent buildings. Such vibrations, especially in high-rise buildings, can lead to physiological effects, such as dizziness, nausea, motion sickness, drowsiness, reduced productivity and headaches, along with psychological effects like anxiety, depression, loss of concentration and fear (Burton et al., 2006; GoTo, 1983; Hansen, 2007; Hansen et al., 1973; Lamb et al., 2013). Therefore, acceleration criteria, often referred to as comfort criteria, are crucial for maintaining acceptable vibration levels. Assessing comfort is inherently subjective. Unlike the mandatory Ultimate Limit State (ULS) criteria, comfort criteria are generally presented as recommendations in building design regulations or as evaluation methods in separate codes, making compliance not obligatory.

Fig. 2 illustrates the evaluation curves for comfort criteria from common international standards and codes, as well as from the guidelines specific to the country with the most high-rise timber buildings. Among them, ISO 10137 (2007) (ISO 10137, 2007) and ISO 6897 (1984) (ISO 6897, 1984) are international standards. ALJ-Guidelines (2004) (ALJ-Guidelines, 2004), NBCC-Guidelines (2017) (NBCC-Guidelines, 2017), ASCE 7-22 (ASCE/SEI 7-22, 2022), and AS/NZS 1170.2 (AS/NZS 1170.2, 2021) are guidelines or standards applicable nationwide in Japan, Canada, the United States, and Australia/New Zealand, respectively.

In the evaluation graphs, the horizontal axis represents the building’s

natural frequency, while the vertical axis denotes floor acceleration. Both axes use logarithmic scales with a base of 10. The comfort criterion is not met if the wind-induced vibration acceleration of any floor in the building, in any direction (typically along-wind, across-wind, or torsional), exceeds the acceleration specified by the curve corresponding to the frequency of the vibration mode in the same direction. When evaluating the torsional acceleration of a floor, the equivalent translational acceleration a_e , calculated using formula (1), should be compared with the evaluation curve illustrated in Fig. 2.

$$a_e = r \times A_\theta(t) \tag{1}$$

Here, r represents the distance from the rotational center to the evaluation point, and $A_\theta(t)$ denotes the peak rotational angular velocity at that point.

- ISO 10137 “Bases for design of structures — Serviceability of buildings and walkways against vibrations”: The evaluation curves from ISO 10137 (2007) (ISO 10137, 2007) are intended explicitly for peak acceleration due to wind-induced vibrations with a one-year return period. It includes separate curves for office buildings and residential buildings, where the acceleration limit for residences is set at two-thirds that of offices. The resultant curve for residences aligns with the 90% perception probability level. The curve decreases monotonically with frequencies below 1 Hz and increases above 2 Hz, with a plateau observed between approximately 1 and 2 Hz at the lowest part of the curve. Notably, ISO 10137 only provides graphical curves without accompanying formulas or numerical tables, which can complicate comparisons and assessments during the design process. In contrast, the NBCC-Guideline (Structural Commentaries User’s Guide - NBC, 2015: Part 4 of Division B) (NBCC-Guidelines, 2017) offers fitted curves for the ISO 10137 standard in the frequency range below 1 Hz. These are expressed as formula (2) (for offices) and formula (3) (for residential buildings), where a_{cri} represents the acceleration evaluation criterion in units of 10 cm/s^2 , f_n is the vibration frequency in Hz, and f_n must be less than 1 Hz. Additionally, ISO 10137 (2007) (ISO 10137, 2007) states that in more complex scenarios, a combination of modal responses may be necessary, though the method for such combinations is not specified. Moreover, since the basic wind speed defined in Eurocode 1-4 (Eurocode 1-4, 2010) corresponds to a 50-year return period,

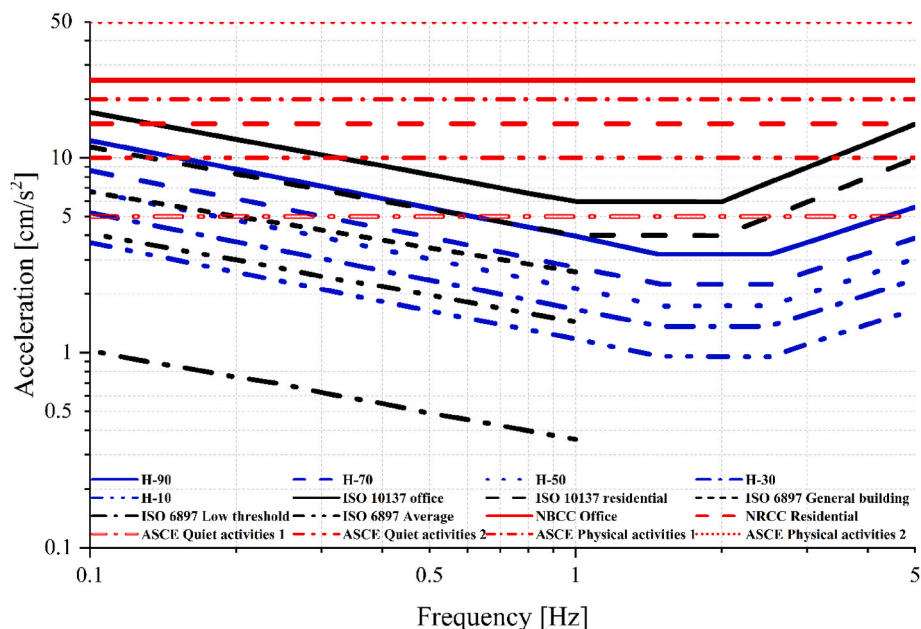


Fig. 2. The evaluation curves of comfort criteria from different standards, codes and guidelines.

and the adjustment formula for return periods provided by the code is not applicable for a 1-year return period, an additional reduction factor is required. For reference, the Guide for the Assessment of Wind Actions and Effects (CNR-DT 207/2008, 2010) on Structures by the National Research Council of Italy recommends a reduction factor of 0.75 for converting 50-year return wind speeds to 1-year return levels.

$$a_{cri} = 0.61 \times f_n^{-0.454} \quad (2)$$

$$a_{cri} = 0.41 \times f_n^{-0.454} \quad (3)$$

- ISO 6897 “Guidelines for the evaluation of the response of occupants of fixed structures, especially buildings and off-shore structures, to low-frequency horizontal motion (0,063 to 1 Hz)”: The standard ISO 6897 (1984) (ISO 6897, 1984) proposed a guideline of root mean square (RMS) acceleration limits for fixed structures, particularly buildings, with vibration frequencies ranging only from 0.063 Hz to 1 Hz. It offers three evaluation curves for assessing wind-induced vibration. The curve named “General” defines acceptable acceleration levels for motion, ensuring that no more than 2% of the building’s occupants are likely to perceive vibrations during the most severe continuous 10-min storm, which has a return period of at least five years. This guideline is applicable for buildings designed for general purposes. The curve named “Average” represents the threshold at which horizontal motion is typically perceived by most adults. It is suitable for buildings where precision activities are conducted. The curve named “Low threshold” identifies the minimum horizontal motion detectable by humans and is appropriate for environments that require an almost motionless setting. The acceleration level of the Average curve is four times higher than that of the Low threshold curve. The standard provides data through tables and figures to simplify the evaluation process. It also suggests that if the probable adverse comment level of a storm with a one-year return period needs to reach 2%, the recommended satisfactory acceleration amplitude should be 0.72 times that of a storm with a five-year return period. Some researchers multiply the RMS value of building acceleration given in the standard by $\sqrt{2}$ (Wijesooriya et al., 2023; Tamura, 2003) or 3.5 (Tamura, 2003; Howarth, 2015) to estimate and compare it with the peak acceleration of the building.
- AIJ-Guideline: The Architectural Institute of Japan (AIJ) proposed the AIJ-Guideline “Guidelines for the evaluation of habitability to building vibration.” (2004) (AIJ-Guidelines, 2004) for evaluating the habitability of buildings. Instead of providing a recommended criterion, it offers five curves for one-year-return peak acceleration: H-10, H-30, H-50, H-70, and H-90. The numbers in the curve names indicate the probability of perception, which represents the percentage of people likely to feel the vibration (e.g., H-10 corresponds to a 10% likelihood). These curves span a vibration frequency range of 0.1 Hz–5 Hz, and their profile is similar to that of ISO 10137 (ISO 10137, 2007). However, the lower end of their frequency range is positioned between approximately 1.5 Hz and 2.5 Hz, which differs from the ISO 10137 standard, which is 1.0 Hz and 2.0 Hz. The AIJ-Guidelines (2004) (AIJ-Guidelines, 2004) emphasizes that building owners should determine the habitability standard for vibration. In contrast, earlier versions of the AIJ-Guidelines (1991) (AIJ-Guidelines, 1991) recommended standard levels of the 2%-perception curve for residential buildings and the 3%-perception curve for office buildings. However, the 2004 version (AIJ-Guidelines, 2004) does not specify a recommended standard, which makes it challenging to determine the appropriate vibration level and select a suitable curve as the design target for a specific building.
- NBCC: NBCC-Guideline (Structural Commentaries User’s Guide - NBC, 2015: Part 4 of Division B) (2017) (NBCC-Guidelines, 2017),

published by the National Research Council of Canada (NRCC) as Structural Commentaries for the National Building Code of Canada (2015) (NBCC, 2018 (NBCC, 2018)), addresses criteria for wind-induced vibrations. While these guidelines do not provide explicit recommendations, they highlight two key points for design reference: Firstly, between 1975 and 2000, many high-rise buildings in North America were tested in wind tunnels using 10-year return winds. Residential buildings were designed to limit peak accelerations to 1.5% of gravitational acceleration (15 cm/s^2), while office buildings were designed for 2.5% of gravitational acceleration (25 cm/s^2). Generally, these designs perform satisfactorily according to these criteria. The two limits for residential and office buildings, which are independent of building vibration frequency, are shown in Fig. 2 as two horizontal lines parallel to the x-axis (solid line for office buildings and dash line for residential buildings). Secondly, for designs based on one-year return wind data, the guide refers to ISO 10137 (ISO 10137, 2007) as the applicable standard. The evaluation criterion of ISO 10137 (ISO 10137, 2007) are based on the 10-min mean wind speed with a one-year return period, whereas the wind speeds provided by NBCC are typically given as hourly mean wind speed for 50-year or 10-year return periods. To align with ISO 10137’s evaluation method, the NRCC guide introduces formula (4), which allows for the conversion of NBCC wind speeds to the equivalent 10-min mean wind speed for a one-year return period. In this formula, $V_{10-min,1}$ represents the 10-min mean wind speed in a one-year return period, while V_{50} and V_{10} correspond to the hourly mean wind speeds for the 50-years and 10-years return periods, respectively.

$$V_{10-min,1} = 1.06 \times [V_{10} - 1.45 \times (V_{50} - V_{10})] \quad (4)$$

- ASCE: ASCE/SEI 7-22 “Minimum Design Loads and Associated Criteria for Buildings and Other Structures” (ASCE/SEI 7-22, 2022), an American national standard published by the American Society of Civil Engineers, establishes minimum design loads for buildings and other structures, that are subject to building code requirements. Its appendix on serviceability considerations highlights the importance of designing structural systems to prevent discomfort caused by wind-induced vibrations to occupants. The commentary appendix provides general guidance on vibration serviceability. It states that sustained vibrations lasting several minutes with accelerations between 0.005 g and 0.01 g (i.e., approximately 5–10 cm/s^2) are likely to annoy individuals engaged in quiet activities. In contrast, individuals involved in physical activities or spectator events may tolerate steady-state accelerations ranging from 0.02 g to 0.05 g (i.e., approximately 20–50 cm/s^2). Furthermore, the commentary stresses that the criteria for building serviceability should be negotiated between the design team and the building owner.
- AS/NZS 1170.2: AS/NZS 1170.2 “Australian/New Zealand Standard-Structural Design Action Part 2: Wind actions” (AS/NZS 1170.2, 2021) serves as the national standard for wind loads in structural design in New Zealand and Australia. Its appendix addresses the acceleration and rotational velocity of wind-sensitive structures, providing a formula (5) to assess whether the wind-induced vibration acceleration of a building exceeds acceptable levels. In this formula, h_{ave} represents the average height of the building roof above ground in meters, and m_0 denotes the average mass per unit height. However, the formula does not account for variations in material stiffness of building, which may limit its applicability for evaluating light-weight timber frame buildings. The standard also references ISO 10137 (ISO 10137, 2007) for assessing maximum acceptable peak acceleration. For wind-induced structural torsion, the appendix specifies a limit for the annual maximum peak rotational velocity, set at 1.5 mrad/s, instead of using acceleration.

$$h_{ave}^{1.3} / m_0 > 0.0016 \quad (5)$$

Excessive vibration amplitudes can damage nonstructural elements, such as cladding, which may impair functionality by preventing doors or windows from opening properly. For this reason, it is crucial to establish limits on building lateral deformation, known as deflection criteria, within Serviceability Limit State (SLS) guidelines. The criteria for SLS deflection under wind loads, as outlined in various codes and guidelines, are summarized in Table 1. These criteria are typically based on story drift, which is defined as the lateral deflection of one-story relative to the story below. For walls, windows, and glazing systems, deflection control may also be based on mid-height or mid-span deflection. Drift limitations are usually expressed as a ratio relative to the story height, such as $h/500$, where h is the floor or building height (in meter). The ASCE 7–22 (ASCE/SEI 7-22, 2022) also recommends an absolute story drift value of 10 mm to prevent damage to nonstructural elements like partitions, cladding, and glazing. While such limitations are often presented as non-mandatory guidelines, some, such as those in the NBCC (NBCC, 2018), are explicitly specified. Deflection criteria for wind-induced vibrations are usually not included in wind action codes but are instead found in general structural design sections, such as AS/NZS 1170.0 (AS/NZS 1170.0, 2002) which covers structural design principles, and in Eurocode 5 (EN, 1995-1-1:2005/A2:2014, 2014), which provides design methods and requirements for timber structures. It should also be recognized that wind-load and combinations for SLS deflection checks can differ from those used for ULS checks. It may sometimes require consultation with the client to establish appropriate serviceability limits.

This section examines the serviceability and deflection criteria used to evaluate wind-induced vibration in high-rise buildings. Most of these criteria are advisory rather than mandatory, making selections difficult. Moreover, each set of limits is tied to a specific wind-return period, and no reliable procedure is provided for converting the resulting accelerations or displacements to other return periods. ISO 10137 (ISO 10137, 2007) notes that combined along-, across-, and torsional responses should be considered; However, it provides no practical method for getting combining amplitudes of effects or vibration frequencies, making such evaluations difficult to perform in practice.

3. Design methods for wind-induced vibration in buildings based on codes/standards

As this study addresses wind-induced vibrations in timber structures, this section focuses on the calculation methods for building vibration responses based on various standards and codes. The standards/codes of AIJ-RLB (2004) (AIJ-RLB, 2004), NBCC (2018) (NBCC-Guidelines, 2017; NBCC, 2018), ASCE 7–22 (2022) (ASCE/SEI 7-22, 2022), AS/NZS 1170.2 (2021) (AS/NZS 1170.2, 2021) and Eurocode 1-4 (2010) (Eurocode 1-4, 2010) are selected to be discussed based on the same reason as mentioned in section of Design criteria. The current version of Eurocode 1–4 is from 2010, while a new draft of Eurocode 1–4 (Eurocode 1-4, 2024) was released in 2024. However, as of the time of writing, the 2024 draft has not yet been officially implemented. In this section, the calculation provisions from both the 2010 version (Eurocode 1-4, 2010) and the 2024 draft of Eurocode 1–4 (Eurocode 1-4, 2024) are compiled and discussed. Although Eurocode 5 (EN, 1995-1-1:2005/A2:2014, 2014) specifically addresses timber structure design and includes a section on vibration design, most of its provisions pertain to the vibration performance of timber floors. These are not relevant to the wind-induced vibration issues discussed in this paper and are therefore not presented here.

The responses considered include wind-induced vibration acceleration and displacement in the along-wind, across-wind and torsional directions. This section further discusses methods for combining accelerations from different directions. For a quick estimation, it also reviews methods for estimating natural frequency and damping values in the last part of this section.

Once the wind-induced vibration response of a timber building is calculated, it can be compared against the ULS- and, particularly, the SLS-criteria to evaluate whether the building design meets the design expectations. To keep this concise, only minimal explanations are provided for each standard's or code's formulas. For definitions of common parameters such as wind speed, reference height and turbulence intensity, please refer to the respective standards and codes directly.

Table 1
Summary of deflection criteria drawn from the codes and standards.

Element/ Structure	Phenomenon controlled	Load combination	Serviceability parameter	Limit	Mandatory	Origin
Building	–	Service wind + gravity loads	Total drift per story	$h/500$	Yes	NBCC (NBCC, 2018)
Bracing system	–	Internal stability load per unit length + External load	Horizontal deflection of the bracing system	$L/500$	Yes	Eurocode 5 (EN, 1995-1-1:2005/A2:2014, 2014)
Building	No damage to cladding, nonstructural walls and partitions.	Dead load + 0.5 Live load + Wind load*	Total drift/Total drift per story	$h/600$ to $h/400$	No	ASCE 7–22 (ASCE/SEI 7-22, 2022)
Columns	Side sway	Wind load with the combination factor of short-term effect specified in AS/NZS 1170.0 (AS/NZS 1170.0, 2002)	Absolute story drift	10 mm	No	AS/NZS 1170.0 (AS/NZS 1170.0, 2002)
Wall-general (face loaded)	Discerned movement		Deflection at top	$h/500$		
Brittle cladding (ceramic) face loaded	Supported elements rattle		Mid-height deflection	$h/150$		
Masonry walls (in plane)	Cracking		Mid-height deflection	$h/1000$		
Masonry walls (face loaded)	Noticeable cracking		Deflection at top	$h/600$		
Plaster/gypsum walls (in plane)	Lining damage		Mid-height deflection	$h/400$		
Plaster/gypsum walls (face loaded)				$h/300$		
Glazing systems	Bowing		Mid-height deflection	$h/200$		
Windows, facades, curtain walls	Facade damage		Mid-span deflection	$S/400$		
			Mid-span deflection	$S/200$		

h : Story or building height (in meter). S : Span of the controlled element/structure. L : Overall length of the stabilizing system.

*The selection of the mean recurrence interval (MRI) for wind in serviceability evaluations is a matter of engineering judgment and should be determined in consultation with the building client.

3.1. Along-wind acceleration

All codes and standards investigated in this section provide formulas to predict the maximum along-wind vibration acceleration of the building. The Commentary part of ASCE 7-22 (2022) (ASCE/SEI 7-22, 2022) (hereafter referred to as ASCE), Annex B and Annex C of Eurocode 1-4 (2010) (Eurocode 1-4, 2010) (hereafter referred to as Eurocode B and Eurocode C), Annex F of new draft of Eurocode 1-4 (2024) (Eurocode 1-4, 2024) (referred to as New Eurocode F), AIJ-RLB (2004) (AIJ-RLB, 2004) (referred to as AIJ), and AS/NZS 1170.2 (2021) (AS/NZS 1170.2, 2021) (referred to as AS/NZS) contain formulas for calculating maximum along-wind acceleration at different heights of buildings.

These formulas are based on gust theory (Davenport, 1962), which employs a simplified frequency-domain approach. In this method, the standard deviation of wind load and dynamic response amplitude are multiplied by a peak factor derived from random vibration theory to estimate the peak response. ASCE (ASCE/SEI 7-22, 2022), Eurocode B (Eurocode 1-4, 2010), Eurocode C (Eurocode 1-4, 2010), New Eurocode F (Eurocode 1-4, 2024), AIJ (AIJ-RLB, 2004) utilize similar formulas to calculate the mean value of along-wind acceleration along the height of the structure and can be expressed as equation (6), where $\overline{\hat{x}}(z)$ is the standard deviation of acceleration in x -axial (along-wind) direction at the point with the height of z , ρ is the air density, \overline{V}_z is the mean wind velocity at the reference height \overline{z} , b is the building width (horizontal dimension of a building measured normal to the wind direction) and h represents the building height, I_z is intensity of turbulence at the reference height \overline{z} , $R_{eff,x}$ represents the effective resonant response factor for along-wind response, $C_{f,x}$ represents the wind force coefficient, K is the mode shape correction factor, $\phi_{1,x}(z)$ represents the fundamental mode shape in the x -axial (along-wind) direction evaluated at height z and $m_{1,x}$ represents generalized mass for along-wind vibration.

$$\overline{\hat{x}}(z) = \frac{\frac{1}{2}\rho\overline{V}_z^2bhC_{f,x}I_zR_{eff,x}K}{m_{1,x}}\phi_{1,x}(z) \quad (6)$$

The AS/NZS (AS/NZS 1170.2, 2021) applies a slightly different formula that uses base bending to account for along-wind effects, which combine both windward and leeward influences, as shown in equation (7), where \overline{M}_{al} is the deviation of resonant along-wind base moment, the reference height \overline{z} is the building height h . $C_{fig,windward}$ and $C_{fig,leeward}$ are windward and leeward force coefficient, respectively.

$$\overline{\hat{x}}(z) = \phi_{1,x}(z) \left\{ \frac{\overline{M}_{al}}{hm_{1,x}} = \frac{I_zR_{eff,x}K}{hm_{1,x}}\phi_{1,x}(z)\rho \left[C_{fig,windward} \sum_{z=0}^h [\overline{V}^2(z)b(z)zdz] - C_{fig,leeward} \overline{V}_z^2 \sum_{z=0}^h [b(z)zdz] \right] \right\} \quad (7)$$

For ASCE (ASCE/SEI 7-22, 2022), Eurocode B (Eurocode 1-4, 2010), Eurocode C (Eurocode 1-4, 2010), New Eurocode F (Eurocode 1-4, 2024), AIJ (AIJ-RLB, 2004), and AS/NZS (AS/NZS 1170.2, 2021), the mean along-wind acceleration could be further multiplied by a peak factor g_r using equation (8), yielding the wind-induced peak acceleration $\hat{x}(z)_{max}$ in the along-wind direction at height z . The method for determining the peak factor g_r is provided in Table 3, where T is the averaging time, and v is the up-crossing rate. Assuming a narrow-banded Gaussian process, v is approximately equal to the building's natural frequency of the first mode in calculated wind direction (n_1). Compared to the 2010 version of Eurocode 1-4 (Eurocode 1-4, 2010), the calculation method for along-wind acceleration in the New Eurocode F (Eurocode 1-4, 2024) remains largely unchanged, with only minor revisions to the effective

resonant response factor, mode shape correction factor and peak factor.

$$\hat{x}(z)_{max} = \overline{\hat{x}}(z)g_r \quad (8)$$

NBCC (NBCC, 2018) and NBCC-Guidelines (NBCC-Guidelines, 2017) offer a formula for calculating peak along-wind acceleration using the building's maximum along-wind deflection (Equation (9)). Because the NBCC-Guidelines serve as commentary to the NBCC and their calculation formulas reference parameters defined in the NBCC, both documents are treated collectively as "NBCC" in this study from here on. On the other hand, the NBCC (NBCC-Guidelines, 2017; NBCC, 2018) does not offer a direct formula for determining the maximum along-wind deflection, which necessitates further structural analysis. This makes it challenging to directly calculate along-wind acceleration of a building using the NBCC.

$$\hat{x}_{max} = 4\pi n_{1,x}^2 g_r \sqrt{\frac{ksF}{C_{eh}\beta_x}} \frac{\Delta_{max}}{\left[1 + g_r \sqrt{\frac{k}{C_{eh}} \left(B + \frac{sF}{\beta_x} \right)} \right]} \quad (9)$$

Where:

\hat{x}_{max} : wind-induced peak acceleration in along-wind direction

$n_{1,x}$: natural frequency of the first mode in along-wind direction

g_r : peak factor for along-wind effect, see Table 3

k : terrain factor, $k = 0.08$ for open terrain and $k = 0.1$ for rough terrain

s : size reduction factor, $s = \frac{\pi}{3} \left[1 / \left(1 + \frac{8hn}{3\overline{V}_z} \right) \right] \left[1 / \left(1 + \frac{10b_{eff}n}{\overline{V}_z} \right) \right]$,

reference height \overline{z} is equal to the building height h , b_{eff} is effective width of windward face of the building and should be calculated as $b_{eff} = \sum_{i=1}^n \frac{b_i h_i}{h_i}$, where, b_i is width normal to wind direction at height h_i , n is the lowest natural frequency of the building

F : gust energy ratio calculated as $F = N_1^2 / (1 + N_1^2)^{4/3}$, where $N_1 = 1220n / \overline{V}_z$

C_{eh} : exposure factor, $C_{eh} = (h/10)^{0.28}$ for open terrain (but $1.0 \leq C_{eh} \leq 2.5$) and, $C_{eh} = 0.5(h/12.7)^{0.5}$ for rough terrain (but $0.5 \leq C_{eh} \leq 2.5$)

β_x : the damping ratio in along-wind direction, which should be determined by a rational method or may be assumed as 0.01 for steel structures, 0.02 for concrete structures, and 0.015 for composite structures

B: background turbulence factor, the value of B is presented as curves in a figure, derived according to formula $B =$

$$4/3 \int_0^{914/h} \left[\frac{1}{1+457x} \right] \left[\frac{1}{1+\frac{x}{122}} \right] \left[\frac{x}{(1+x^2)^{4/3}} \right] dx$$

Δ_{max} : maximum along-wind lateral deflection at the top of the building

In summary, all of the preceding along-wind-acceleration formulations account only for the fundamental along-wind mode. Yet several studies have shown that excluding higher modes can lead to an under-estimation of wind-induced response, particularly in tall, lightweight structures (Feng et al., 2012; Aly, 2013). Because timber buildings have comparatively low mass, their higher modes often remain in the

Table 2
Summary of values or calculation methods for parameters in along-wind acceleration equations.

Standard/Code	$R_{eff,x}$	$C_{f,x}$	K	$\phi_{1,x}(z)$	$m_{1,x}$
ASCE (ASCE/SEI 7-22, 2022)	$1.7\sqrt{\frac{1}{\beta_x}R_nR_hR_b(0.53+0.47R_d)}$ see note ¹	Along-wind force coefficient ²	$\frac{1.65^{\bar{\alpha}}}{\bar{\alpha} + \xi + 1}$	$(z/h)^\xi$	$\int_0^h \mu(z)\phi_{1,x}^2(z)dz$
Eurocode B (Eurocode 1-4, 2010)	$\frac{2}{h}\sqrt{\frac{\pi^2}{2\delta_x}R_nR_hR_b}$ see note ³	Along-wind force coefficient ⁴	$\int_0^h \bar{V}^2(z)\phi_{1,x}(z)dz$ or $\bar{V}^2(z)\int_0^h \phi_{1,x}^2(z)dz$ approximation ⁵	$(z/h)^\xi$ see note ⁶	$\int_0^h \mu(z)\phi_{1,x}^2(z)dz$ or $\int_0^h \phi_{1,x}^2(z)dz$ approximation ⁷
Eurocode C (Eurocode 1-4, 2010)	$\frac{2}{bh}\sqrt{\frac{\pi^2}{2\delta_x}R_nK_s(n_{1,x})}$ see note ⁸	Along-wind force coefficient ⁴	$\frac{3}{2\phi_{max}}$ see note ⁹	z/h	$\int_0^h \int_0^b \mu(y,z)\phi_{1,x}^2(y,z)dydz$ or $\int_0^h \int_0^b \phi_{1,x}^2(y,z)dydz$ approximation ¹⁰
AIJ (AIJ-RLB, 2004)	$\sqrt{\frac{\pi}{4\beta_x}FS_D(0.57-0.35\xi+2R_b\sqrt{0.053-0.042\xi})}$ see note ¹¹	$C_{pe1} - C_{pe2}$ or given in Table 12	$1 - 0.4 \ln \xi$	$(z/h)^\xi$	$\int_0^h \mu(z)\phi_{1,x}^2(z)dz$
AS/NZS (AS/NZS 1170.2, 2021)	$\sqrt{\frac{SE_t}{\beta_x}(1+6.8I_z)}$ see note ¹³	See note ¹⁴	1	$(z/h)^\xi$ see note ¹⁵	$\frac{\mu_0 h}{3}$ see note ¹⁶
New Eurocode F (Eurocode 1-4, 2024)	$\frac{2}{h}\sqrt{\frac{\pi^2}{2\delta_x}R_nR_hR_b}$ see note ¹⁷	Along-wind force coefficient ¹⁸	$\frac{\xi+2}{2\phi_{max}}$ see note ¹⁹	$(z/h)^\xi$ see note ⁶	$\int_0^h \mu(z)\phi_{1,x}^2(z)dz$ or $\int_0^h \phi_{1,x}^2(z)dz$ approximation ⁷

Note: β_x : Damping ratio in along-wind direction expressed as percent of critical damping; δ : Logarithmic decrement of damping; $n_{1,x}$: Natural frequency of the first mode in along-wind direction; L_z : integral length scale of turbulence at the reference height \bar{z} ; $\bar{\alpha}$: mean hourly wind-speed power law exponent; ξ : mode shape exponential coefficient; $\mu(z)$: mass per unit height at height z .

*1: $R_n = \frac{7.47N_1}{(1+10.3N_1)^{5/3}}$, $N_1 = \frac{n_{1,x}L_z}{V(\bar{z})}$, $R_l = \frac{1}{\eta} - \frac{1}{2\eta^2}(1 - e^{-2\eta})$, where $l = h, b, d$ (d is the horizontal dimension of a building measured parallel to the wind direction),

when $R_l = R_h$ then $\eta = 4.6n_{1,x}h/\bar{V}_z$, when $R_l = R_b$ then $\eta = 4.6n_{1,x}b/\bar{V}_z$, $R_l = R_d$ then $\eta = 15.4n_{1,x}d/\bar{V}_z$

*2: The value is given in tabular form and depends on factors such as the shape of the structure, the height above ground level and building width to height ratio etc.

*3: δ_x is the logarithmic decrement of total damping in along-wind direction. $\delta_x = \delta_{x,s} + \delta_{x,a} + \delta_{x,d}$, where $\delta_{x,s}$ is the logarithmic decrement of structural damping in along-wind direction, $\delta_{x,a}$ is the logarithmic decrement of aerodynamic damping for the fundamental mode in along-wind direction and $\delta_{x,d}$ is the logarithmic decrement of damping due to special devices in along-wind direction. The following formula is given to estimate the $\delta_{x,a}$ for buildings: $\delta_{x,a} = \frac{\rho\bar{V}_z b C_{f,x}}{2m_{1,x}n_{1,x}}$; Approximate values for $\delta_{x,s}$ are provided in tabular form according to structural type. No specific value is listed for timber buildings. However, for timber bridges, a range of 0.06–0.12 is indicated; $R_n = \frac{6.8N_1}{(1+10.2N_1)^{5/3}}$, $N_1 = \frac{n_{1,x}L_z}{V(\bar{z})}$, $R_l = \frac{1}{\eta} - \frac{1}{2\eta^2}(1 - e^{-2\eta})$, where $l = h, b$, when $R_l = R_h$ then $\eta = 4.6n_{1,x}h/\bar{V}_z$, when $R_l = R_b$ then $\eta = 4.6n_{1,x}b/\bar{V}_z$.

*4: The coefficient is presented as curves in various figures, with the choice of figures determined by the building shape. For a standard rectangular building, the curve plots the building's aspect ratio on the horizontal axis and the coefficient on the vertical axis. The corresponding definition formula for the curve is also provided.

*5: When the mode shape $\phi_{1,x}(z) = (z/h)^\xi$ is assumed and flat terrain condition is met, it can be approximated as: $\frac{(2\xi+1) \cdot \left\{ (\xi+1) \cdot \left[\ln\left(\frac{z}{z_0}\right) + 0.5 \right] - 1 \right\}}{(\xi+1)^2 \cdot \ln\left(\frac{z}{z_0}\right)}$, where z_0 is

the roughness length, which depends on the terrain category and is provided in tabular form in the standard.

*6: The suggestions for the value of ξ are given in the code as: 0.6 for slender frame structures featuring non-load-sharing walling or cladding, 1.0 for buildings featuring a central core plus peripheral columns, or larger columns plus shear bracings, 1.5 for slender cantilever buildings and those supported by central reinforced concrete cores, 2.0 for towers and chimneys etc.

*7: For cantilevered structures (e.g., buildings) with varying mass distributions, it can be approximated by the average mass of the upper third of the structure.

*8: For the calculation of δ_x and R_n , refer to Note 3; $K_s(n_{1,x})$ is size reduction function based on the building natural frequency of the first mode in along-wind direction

$(n_{1,x}), K_s(n_{1,x}) = 1/\left(1 + \sqrt{\left(\frac{1}{2}\phi_y\right)^2 + \left(\frac{3}{8}\phi_z\right)^2 + \left(\frac{3}{8\pi}\phi_y\phi_z\right)^2}\right)$, where $\phi_y = \frac{11.5bn_{1,x}}{\bar{V}_z}$ and $\phi_z = \frac{11.5hn_{1,x}}{\bar{V}_z}$.

*9: ϕ_{max} is the mode shape value at the point with maximum amplitude, which should be 1 since linear vertical mode shape is assumed in this case for building.

*10: It can be approximated as the mass per unit area of the structure at the point of the largest amplitude of the mode shape. $\mu(y, z)$ is mass per unit area at the height z and width y .

*11: $F = \frac{4N_1}{(1+71N_1^2)^{5/6}}$, $N_1 = \frac{n_{1,x}L_z}{V(\bar{z})}$, $S_D = 0.9/\left\{\left[1 + 6\left(\frac{hn_{1,x}}{\bar{V}_z}\right)^2\right]^{0.5} \left(1 + 3\frac{bn_{1,x}}{\bar{V}_z}\right)\right\}$, $R_b = 1/\left(1 + 20\frac{bn_{1,x}}{\bar{V}_z}\right)$.

*12: For a rectangular building, $C_{fx} = C_{pe1} - C_{pe2}$, where C_{pe1} and C_{pe2} are the external pressure coefficients on the windward and leeward faces, respectively, provided in tabular form. For other structural shapes, such as circular or lattice configurations, the corresponding value of C_{fx} values are also presented in tables.

*13: S is size reduction factor, $S = 1/\left[\left(1 + 3.5\frac{hn_{1,x}(1+3.4I_z)}{\bar{V}_z}\right)\left(1 + 4\frac{b_0n_{1,x}(1+3.4I_z)}{\bar{V}_z}\right)\right]$, where b_0h represents the average breadth of the structure from height

0 up to height h . $E_t = \frac{\pi N}{(1+70.8N^2)^{5/6}}$, $N = \frac{n_{1,x}L_z}{V(\bar{z})}(1+3.4I_z)$.

*14: In this code, the influence of wind on a building in the along-wind direction is divided into windward and leeward effects. Instead of $C_{f,x}$, two separate coefficients are used for the calculation: $C_{fig.windward}$ for the external aerodynamic shape factor on the windward surface and $C_{fig.leeward}$ for the external aerodynamic shape factor on the leeward surface. For enclosed building, both coefficients can be calculated by following equation: $C_{fig.windward}$ or $C_{fig.leeward} = C_{p,e}K_aK_{c,e}K_lK_p$, where $C_{p,e}$, K_a , $K_{c,e}$, K_l and K_p are external pressure coefficient, area reduction factor, combination factor, local pressure factor and porous cladding reduction factor, respectively. Their values are provided in tabular form in the standard/code.

*15: The value of ξ can be determined either by fitting the mode shape derived from modal analysis, or by following recommended values: 1.5 for a uniform cantilever; 0.5 for a moment-resistant slender frame structure; 1.0 for a building with central core and moment-resistant facade; 2.3 for a tower decreasing in stiffness with height or with large mass at top.

*16: It is assumed that mass per unit height $\mu(z)$ at any z is identical and equal to μ_0 .

*17: For the calculation of δ_x refer to Note 3; $R_n = \frac{6.8N_1}{(1 + 10.2N_1)^{5/3}}$, $N_1 = \frac{n_{1,x}L_z}{\sqrt{V_z}}$, $R_l = \frac{2}{\eta^2}(\eta - 1 + e^{-\eta})$, where $l = h, b$, when $R_l = R_h$ then $\eta = 8.6n_1h/\sqrt{V_z}$, when $R_l = R_b$ then $\eta = 8.6n_{1,x}b/\sqrt{V_z}$.

*18: The coefficient is presented as curves in various figures, with the choice of figure determined by the building shape. For a standard rectangular building, the curve plots the building's aspect ratio on the horizontal axis and the coefficient on the vertical axis, with no difference with the old version of the Eurocode 1-4 (2010) (Eurocode 1-4, 2010).

*19: ϕ_{max} is the mode shape value at the point with maximum amplitude. The suggestions for the value of ξ please see note 6.

Table 3

Summary of calculation methods of peak factor for wind-induced effect from the codes and standards.

	ASCE (ASCE/SEI 7-22, 2022)	Eurocode B/C (Eurocode 1-4, 2010)	New Eurocode G/F/H (Eurocode 1-4, 2024)	AIJ (AIJ-RLB, 2004)	AS/NZS (AS/NZS 1170.2, 2021)	NBCC (NBCC, 2018)
g	$\sqrt{2 \ln(vT)} + \frac{0.5772}{\sqrt{2 \ln(vT)}}$	$\sqrt{2 \ln(vT)} + \frac{0.6}{\sqrt{2 \ln(vT)}}$	$\sqrt{2 \ln(vT)} + \frac{0.5772}{\sqrt{2 \ln(vT)}}$	$\sqrt{2 \ln(vT)} + 1.2$	$\sqrt{2 \ln(vT)} + 1.2$	$\sqrt{2 \ln(vT)} + \frac{0.577}{\sqrt{2 \ln(vT)}}$
T	3600 [s]	600 [s]	600 [s]	600 [s]	600 [s]	3600 [s]
ν	n_1	$n_1 \sqrt{\frac{R^2}{R^2 + B^2}}$ see note 1	$n_{1,x}$ or $2n_{1,y}$ or $2n_{1,t}$	n_1	n_1	$n_1 \sqrt{\frac{sF}{sF + B\beta}}$ see note 2

Note: n_1 is the natural frequency of the first mode in the calculated direction ($n_{1,x}$ for along-wind, $n_{1,y}$ for across-wind or $n_{1,t}$ for torsional directions).

1: R represents the resonant response factor. For Eurocode B, $R = \sqrt{\frac{\pi^2}{2\delta} R_n R_h R_b}$, please see note 3 on Table 2. For Eurocode C, $R = \sqrt{\frac{\pi^2}{2\delta_x} R_n K_s (n_{1,x})}$, please see note 8 on

Table 2. B is background factor, $B = \sqrt{1 / \left[1 + 0.9 \left(\frac{b+h}{L_z} \right)^{0.63} \right]}$ for Eurocode B and $B = \sqrt{1 / \left(1 + 1.5 \sqrt{\left(\frac{b}{L_z} \right)^2 + \left(\frac{h}{L_z} \right)^2 + \left(\frac{h}{L_z} \frac{b}{L_z} \right)^2} \right)}$ for Eurocode C, respectively.

Using $B = 1$ provides a conservative estimate.

2: β is damping ratio in the calculated wind direction. Please see the note of equation (9).

low-frequency range and can meaningfully amplify acceleration. Field measurements of Mjøstårnet building in Norway (Tulebekova et al., 2022), for example, record a second-order mode at roughly 0.5 Hz (first mode in the direction parallel to the short edge) and a fourth-order mode near 1.9 Hz (Tulebekova et al., 2022) (second mode in the direction parallel to the short edge)—both below the 5 Hz threshold commonly associated with perceptible vibration. These observations underscore the need for refined design guidance that explicitly addresses higher-mode contributions to wind-induced vibration in high-rise timber buildings.

3.2. Across-wind acceleration

Due to lighter self-weight and lower elastic modulus compared to reinforced concrete or steel, high-rise timber structures could exhibit a lower natural frequency in the across-wind direction than those of reinforced concrete or steel buildings. This characteristic makes light-weight timber buildings prone to resonance with vortex shedding frequencies. Consequently, the across-wind acceleration of high-rise timber buildings might become sufficiently large to exceed along-wind acceleration. However, among the standards/codes examined, only four, i.e., NBCC (NBCC-Guidelines, 2017; NBCC, 2018), AIJ (AIJ-RLB, 2004), AS/NZS (AS/NZS 1170.2, 2021) and the Annex G and Anne H of new draft Eurocode 1–4 (Eurocode 1-4, 2024) (namely New Eurocode G, New Eurocode H below, respectively), provide equations for calculating crosswind acceleration with conditions.

Table 4 summarizes the conditions for using the across-wind acceleration formulas in these four standards. The NBCC (NBCC-Guidelines, 2017; NBCC, 2018) suggests a non-mandatory condition indicating that a building's across-wind acceleration may exceed its along-wind acceleration. However, this suggestion considers only the building size (length, width and height) and neglects potential variations in natural frequency due to the use of different construction materials. Consequently, it may not accurately reflect the wind effect on high-rise timber buildings. The equations for across-wind acceleration in AIJ (AIJ-RLB, 2004), AS/NZS (AS/NZS 1170.2, 2021) and New Eurocode G (Eurocode 1-4, 2024) are limited to buildings with regular dimensions and rectangular cross-sections. In reality, high-rise timber buildings can have irregular cross sections, e.g. 84-m tall HoHo in Vienna Austria (Woschitz, 2015), 73-m tall Haut in Amsterdam (Verhaegh et al., 2020), The Netherlands, 69.7 m-tall 55 Southbank Boulevard in Melbourne, Australia (Nathan, 2019). The AIJ (AIJ-RLB, 2004) requires that three inequalities be satisfied, which account for both geometry and across-wind natural frequency of the building. In contrast, the AS/NZS code (AS/NZS 1170.2, 2021) specifies four inequalities for applying the across-wind acceleration calculation formula. These inequalities are derived from the conditions needed to determine the parameter C_{fs} (see later Table 5, note 2, in this section). They incorporate the building's external dimensions and the reduced velocity V_n , which is calculated from the across-wind natural frequency, wind speed, and turbulence intensity at the reference height. If V_n exceeds $8 [m \cdot s^{-1} \cdot Hz^{-1}]$, the across-wind acceleration equation may still be used, but only for

Table 4
Summary of applicable conditions for the across-wind acceleration equations.

	NBCC (NBCC-Guidelines, 2017; NBCC, 2018)	AIJ (AIJ-Guidelines, 2004)	AS/NZS (AS/NZS 1170.2, 2021)	New Eurocode G (Eurocode 1-4, 2024)	New Eurocode H (Eurocode 1-4, 2024)
Building shape	–	Rectangular cross-section	Rectangular cross-section	Rectangular cross-section	No significant changes on the across-wind dimension ⁵
Dimensions	$\frac{\sqrt{b_{eff}d_{eff}}}{h} < \frac{1}{3}$ see note ¹	$\frac{h}{\sqrt{bd}} \leq 6$ and $0.2 \leq \frac{d}{b} \leq 5$ and $\frac{\bar{V}_z}{n_{1,y}\sqrt{bd}} \leq 10$ see note ²	$2 \leq V_n = \frac{\bar{V}_z}{bn_{1,y}(1+3.4I_z)} \leq 16$ and $0.5 \leq \frac{d}{b} \leq 2$ and $3 \leq \frac{h}{b} \leq 6$ And $3 \leq \frac{h}{d} \leq 6$ see note ³	$3 \leq \frac{h}{\sqrt{bd}} \leq 6$ and $0.2 \leq \frac{d}{b} \leq 5$ and $\frac{\bar{V}_z}{n_{1,y}\sqrt{bd}} \leq 10$ see note ⁴	$8 \leq \frac{h}{\sqrt{bd}}$ and for rectangular building $\frac{1}{3} \leq \frac{d}{b} \leq 2$ see note ⁶

Note.

*1: b_{eff} is effective width of the building (effective horizontal dimension perpendicular to the wind), $b_{eff} = \frac{\sum b_i h_i}{\sum h_i}$, where, b_i is width of building normal to wind direction at height h_i . d_{eff} is effective depth of the building (effective horizontal dimension parallel to the wind), $d_{eff} = \frac{\sum d_i h_i}{\sum h_i}$, where, d_i is depth of building parallel to wind direction at height h_i . h is the height of the building. According to the code, when this condition is satisfied, the across-wind acceleration is likely to exceed the along-wind acceleration. However, meeting this condition is not mandatory for applying the equation.

*2: b is width of the building (horizontal dimensions perpendicular to the wind), d is depth of the building (horizontal dimension parallel to the wind), h is the height of the building (in meter), \bar{V}_z is mean wind velocity at the reference height \bar{z} , $n_{1,y}$ is the natural frequency of the first mode in across-wind direction.

*3: \bar{V}_z is mean wind velocity at the reference height \bar{z} , for this code, the reference height $\bar{z} = h$, $n_{1,y}$ is the natural frequency of the first mode in across-wind direction, I_z is the turbulence intensity at the reference height $\bar{z} = h$, V_n is called reduced velocity. When the V_n is greater than 8, the across-wind acceleration calculated using the provided equation of the code/standard is no longer considered conservative and must be validated through wind tunnel testing.

*4: The explanation of the notation please see note 2. In addition to dimensional requirements, the following conditions must also be met: (1) The wind direction must be orthogonal to the building surface, as this typically represents the most critical scenario; (2) The building must have a uniform vertical mass distribution. When $6 \leq \frac{h}{\sqrt{bd}} \leq 8$, the most severe response should be considered based on the provisions of the New Eurocode G and New Eurocode H.

*5: No specific building shape is required; however, the annex provides parameter values for calculations only for buildings with rectangular, regular hexagon or triangular cross-sections.

*6: b is width of the building (horizontal dimensions perpendicular to the wind), d is depth of the building (horizontal dimension parallel to the wind), h is the height of the building. Besides, the Scruton number S_c ($S_c = \frac{2\delta_s m_{1,y}}{\rho b d}$, the meaning of the notations please see the note of Table 5) of the building should be low. The specific limitations for the Scruton number will be provided in the national annex. When $6 \leq \frac{h}{\sqrt{bd}} \leq 8$, the most severe response should be considered based on the provisions of the New Eurocode G and New Eurocode H.

preliminary design against wind-induced across-wind vibration, then in such cases a wind tunnel testing is required for final confirmation before the formal structural design.

It is noteworthy that both the new drafts of Eurocode (Eurocode 1-4, 2024) and AIJ (AIJ-RLB, 2004) establish requirements for $\frac{h}{\sqrt{bd}}$ value (h , b and d are the height, width and length of the building, respectively, when applying the across-wind acceleration calculation procedure. The parameter represents the building height divided by the geometric mean of its plan dimensions (length and width). As a dimensionless parameter, it reflects the slenderness ratio of the building, larger values correspond to a slenderer building. Therefore, the author would recommend $\frac{h}{\sqrt{bd}}$ as the definition of slenderness ratio of the building. In New Eurocode G (Eurocode 1-4, 2024), the requirements are similar to those in AIJ (AIJ-RLB, 2004), except that the lower bound of the slenderness ratio $\frac{h}{\sqrt{bd}}$ must exceed 3. New Eurocode H (Eurocode 1-4, 2024), designed for slender structures, mandates a slenderness ratio greater than 8. For buildings with a slenderness ratio between 6 and 8, the acceleration should be determined using both New Eurocode G (Eurocode 1-4, 2024) and New Eurocode H (Eurocode 1-4, 2024), with the larger result being adopted.

NBCC’s across-wind acceleration formula (NBCC-Guidelines, 2017; NBCC, 2018), i.e., Equation (10), is empirical, derived from extensive wind tunnel tests (NBCC-Guidelines, 2017). Within this formula, parameter a_r is determined using Equation (11). In both formulas, \hat{y}_{max} represents the maximal across-wind acceleration; $n_{1,y}$ is building’s natural frequency of the first mode in across-wind direction; g_r is the peak factor refers to Table 3; ρ_B is the density of the building; g is the gravitational acceleration constant; β_y is the damping ratio of critical

damping in across-wind direction; \bar{V}_z is the mean wind velocity at the reference height \bar{z} ; b , d , h are the width, depth and height of the building, respectively.

$$\hat{y}_{max} = \frac{n_{1,y}^2 g_r \sqrt{bd} a_r}{\rho_B g \sqrt{\beta_y}} \tag{10}$$

$$a_r = 7.85 \times 10^{-2} \left[\bar{V}_z / (n_{1,y} \sqrt{bd}) \right]^{3.3} \tag{11}$$

AIJ (AIJ-RLB, 2004), AS/NZS (AS/NZS 1170.2, 2021), New Eurocode G (Eurocode 1-4, 2024) and New Eurocode H (Eurocode 1-4, 2024) compute the peak across-wind acceleration by dividing the maximum resonant across-wind overturning moment at the base by the product of the generalized mass and the building height, as shown in Equation (12), where, \hat{y}_{max} represents the maximal across-wind acceleration, $M_{ac,max}$ is the maximal across-wind resonant component of base overturning moment, h is the height of the building and $m_{1,y}$ is the generalized mass of building. $M_{ac,max}$ can be further expanded and expressed in terms of peak factor g_r (see Table 3) air density ρ , mean wind velocity at the reference height \bar{V}_z , the across-wind overturning moment coefficient $C_{f,y}$, the across-wind effective resonance factor $R_{eff,y}$, and the mode correlation factor K_y . The calculations and values for $C_{f,y}$, $R_{eff,y}$, K_y and $m_{1,y}$ are summarized in Table 5.

$$\hat{y}_{max} = \frac{M_{ac,max}}{hm_{1,y}} = \frac{g_r^2 \rho \bar{V}_z^2 b h^2 C_{f,y} R_{eff,y} K_y}{hm_{1,y}} \tag{12}$$

Table 5
Summary of values and calculation methods for parameters in the across-wind acceleration equations.

	$C_{f,y}$	$R_{eff,y}$	K_y	$m_{1,y}$
AIJ (AIJ-Guidelines, 2004)	$0.0082 \frac{d^3}{b^3} - 0.071 \frac{d^2}{b^2} + 0.22 \frac{d}{b}$	$\sqrt{\frac{\pi F_L}{4\beta_y}}$ see note ¹	$1 - 0.4 \ln \xi$	$\int_0^h \mu(z) \phi_{1,y}^2(z) dz$
AS/NZS (AS/NZS 1170.2, 2021)	$R_{eff,y} C_{f,y} = \frac{\sqrt{\frac{\pi C_{fs}}{\beta_y}}}{2(1 + 3.4I_z^2)}$ see note ²		$\frac{3(0.76 + 0.24\xi)}{\xi_1 + 2}$ see note ³	$\frac{\mu_0 h}{3}$ see note ⁴
New Eurocode G (Eurocode 1-4, 2024)	$-0.015 \frac{d^2}{b^2} + 0.14 \frac{d}{b} + 0.03$	$\sqrt{\frac{\pi^2 F_L}{4\delta_{y,s}}}$ see note ⁵	1	$\int_0^h \mu(z) \phi_{1,y}^2(z) dz$
New Eurocode H (Eurocode 1-4, 2024)	Provided as a table, see note ⁶	$\frac{3I_z d}{4h} \sqrt{\frac{\pi^2}{2\delta_y} R_n R_h R_b}$ see note ⁷	3	$\int_0^h \mu(z) \phi_{1,y}^2(z) dz$ or approximation ⁸ $\int_0^h \phi_{1,y}^2(z) dz$

Note: d : depth of building; b : width of building; h : the building height; β_y : the damping ratio in the across-wind direction; ξ : mode shape exponential coefficient for the mode shape in across-wind direction $\phi_{1,y}(z) = \left(\frac{z}{h}\right)^\xi$; \bar{V}_z : mean wind velocity at the reference height \bar{z} ; I_z : the turbulence intensity at the reference height \bar{z} , for both AIJ, AS/NZS, New Eurocode G, $\bar{z} = h$, for New Eurocode H, $\bar{z} = 0.6h$; $\mu(z)$: mass per unit height at height z ; $n_{1,y}$: the natural frequency of the first mode in across-wind direction.

$$*1: F_L = \sum_{j=1}^m \frac{4K_j(1 + 0.6\beta_j)\beta_j}{\pi} \frac{(n_{1,y}/f_{sj})^2}{[1 - (n_{1,y}/f_{sj})^2]^2 + 4\beta_j^2(n_{1,y}/f_{sj})^2}, \text{ where } m = \begin{cases} 1, & (b/d < 3) \\ 2, & (b/d > 3) \end{cases}, K_j = \begin{cases} 0.85, & (j = 1) \\ 0.02, & (j = 2) \end{cases}, f_{s1} = \frac{0.12\bar{V}_z}{b[1 + 0.38(d/b)^2]^{0.89}}, f_{s2} = \frac{0.56\bar{V}_z}{b(d/b)^{0.85}},$$

$$\beta_1 = \frac{(d/b)^4 + 2.3(d/b)^2}{2.4(d/b)^4 - 9.2\left(\frac{d}{b}\right)^3 + 18\left(\frac{d}{b}\right)^2 + 9.5\left(\frac{d}{b}\right) - 0.15} + \frac{0.12}{(d/b)}, \beta_2 = \frac{0.28}{(d/b)^{0.34}}.$$

*2: For $h : b : d = 3 : 1 : 1$ and $2 \leq V_n \leq 16$ and $I_{2/3h} = 0.12$ ($I_{2/3h}$ is the turbulence intensity at height of 2/3 building height h): $\log_{10} C_{fs} = 0.000353V_n^4 - 0.0134V_n^3 + 0.15V_n^2 - 0.345V_n - 3.109$; For $h : b : d = 3 : 1 : 1$ and $2 \leq V_n \leq 16$ and $I_{2/3h} = 0.2$: $\log_{10} C_{fs} = 0.00008V_n^4 - 0.0028V_n^3 + 0.0199V_n^2 + 0.13V_n - 2.985$; For $h : b : d = 6 : 1 : 1$ and $2 \leq V_n \leq 16$: $\log_{10} C_{fs} = 0.00037V_n^4 - 0.0145V_n^3 + 0.17V_n^2 - 0.49V_n - 2.5$; For $h : b : d = 6 : 2 : 1$ and $2 \leq V_n \leq 16$: $\log_{10} C_{fs} = \frac{-0.00045V_n^4 + 0.065V_n^3 - 3.05}{0.00015V_n^4 - 0.018V_n^2 + 1}$; For $h : b : d = 6 : 1 : 2$ and $2 \leq V_n \leq 16$: $\log_{10} C_{fs} = -0.0087V_n^2 + 0.2419V_n - 3.1458$; For intermediate values of $h:b, b:d$, or turbulence intensity, linear interpolation of $\log_{10} C_{fs}$ shall be used. Extrapolation is not permitted.

*3: Based on the calculation equation for the base overturning moment, ξ_1 should theoretically be identical to ξ . However, ξ_1 in the across-wind acceleration equation, is taken as 1. The value of ξ can be determined either by fitting the mode shape derived from modal analysis, or by following recommended values: 0.5 for a moment-resistant slender frame structure; 1.0 for a building with central core and moment-resistant facade; 1.5 for a uniform cantilever; 2.3 for a tower decreasing in stiffness with height or with large mass at top.

*4: It is assumed that mass per unit height $\mu(z)$ at any z is identical and equal to μ_0 .

*5: $\delta_{y,s}$ is the logarithmic decrement of structural damping in across-wind direction. No specific value is listed for timber buildings. However, for timber bridges, a range of 0.06–0.12 is indicated. For the calculation of F_L , please refer to Note 1.

*6: The table provides coefficient values for buildings with triangular, regular hexagonal, or square cross-sections. For buildings with rectangular cross-sections, the coefficient value depends on the aspect ratio of the cross-section. For buildings with square cross-sections, the value is influenced by the sharpness of the corners.

*7: δ_y is the logarithmic decrement of total damping in across-wind direction. $\delta_y = \delta_{y,s} + \delta_{y,a} + \delta_{y,d}$, where $\delta_{y,s}$ is the logarithmic decrement of structural damping in across-wind direction, $\delta_{y,a}$ is the logarithmic decrement of aerodynamic damping for the fundamental mode in across-wind direction and $\delta_{y,d}$ is the logarithmic decrement of damping due to special devices in across-wind direction. The following formula is given to estimate the $\delta_{y,a}$ for buildings: $\delta_{y,a} = \frac{\rho \bar{V}_z d C_{f,y}}{4m_{1,y} n_{1,y}}$; No specific

value for $\delta_{y,s}$ is listed for timber buildings. However, for timber bridges, a range of 0.06–0.12 is indicated; $R_n = \frac{9.4N_1}{(1 + 14.1N_1)^{5/3}}, N_1 = \frac{n_{1,y} L \bar{z}}{4\bar{V}_z}, R_l = \frac{2}{\eta^2}(\eta - 1 + e^{-\eta})$,

where $l = h, b$, when $R_l = R_h$ then $\eta = 4.5n_{1,y}h/\bar{V}_z$, when $R_l = R_b$ then $\eta = 4.5n_{1,y}b/\bar{V}_z$

*8: For cantilevered structures (e.g., buildings) with varying mass distributions, it can be approximated by the average mass of the upper third of the structure.

3.3. Torsional acceleration

Among the codes/standards examined, only AS/NZS (AS/NZS 1170.2, 2021), AIJ (AIJ-Guidelines, 2004) and the Annex G of new draft Eurocode (Eurocode 1-4, 2024) (namely New Eurocode G) provide methods for calculating the rotational acceleration caused by wind-induced vibrations. As noted in Section 2, AS/NZS recommends an upper limit for peak torsional velocity under serviceability limit states (SLS). Accordingly, AS/NZS provides a formula for determining the peak rotational velocity (angular), denoted as equation (13), where $\hat{\theta}_{max}$ is the peak rotational velocity (angular), $n_{1,t}$ is the building's natural frequency of the first mode in torsional direction, $M_{t,max}$ represents the maximum resonant torsional moment, arising from resonant along-wind

forces $F_{res,x}$ with an assumed eccentricity of 0.2 times the building width b , $m_{1,t}$ is generalized inertial moment for torsional vibration, g_r is the peak factor for torsional effect. $F_{res,x}$ is obtained by dividing the resonant base bending moment deviation $\overline{M_{al}}$, due to along-wind effects, by $0.67 \times h$ (where h is the building height). The calculation of $\overline{M_{al}}$ is detailed in Equation (7). The peak factor g_r is referenced in Table 3. While the code AS/NZS (AS/NZS 1170.2, 2021) does not explicitly describe how to calculate the normalized inertial moment $m_{1,t}$, it mentions only that it is derived from floor masses and the normalized mode shape.

$$\hat{\theta}_{max} = 2\pi n_{1,t} \theta = 2\pi n_{1,t} \frac{M_{t,max}}{m_{1,t}} = 2\pi n_{1,t} \frac{0.2bF_{res,x}}{m_{1,t}} = 2\pi n_{1,t} \frac{0.2b\overline{M_{al}}g_r}{0.67hm_{1,t}} \quad (13)$$

Equation (14), as provided in AS/NZS (AS/NZS 1170.2, 2021), computes torsional acceleration $\hat{\theta}_{max}$ using the similar parameter calculations outlined in Equation (13). In addition, it requires r_{max} , which is the distance from the furthest point away from the center of rigidity at the top of the building.

$$\hat{\theta}_{max} = (2\pi n_{1,t})^2 \theta_{r_{max}} = (2\pi n_{1,t})^2 r_{max} \frac{0.2b\overline{M}_{al}g_r}{0.67hm_{1,t}} \quad (14)$$

Formula (15), provided by AIJ (AIJ-Guidelines, 2004) as well as New Eurocode G (Eurocode 1-4, 2024), computes torsional acceleration, where $\hat{\theta}_{max}$ is the peak torsional acceleration, g_r is the peak factor for torsional effect (see Table 3), $C_{f,t}$ represents the torsional moment coefficient, $R_{eff,t}$ denotes the effective resonant factor for torsional effect, K_t is the mode correction factor for torsional effect and $m_{1,t}$ is the generalized inertial moment. The conditions for applying Formula (15) are listed in Table 6 and the calculation methods or values for parameters $C_{f,t}$, $R_{eff,t}$, K_t and $m_{1,t}$ are given in Table 7. Basically, AIJ (AIJ-Guidelines, 2004) and New Eurocode G (Eurocode 1-4, 2024) provide a similar procedure and requirements for calculating torsional acceleration, with the primary difference being how damping is represented. AIJ (AIJ-Guidelines, 2004) expresses damping as a ratio in the formula for computing the effective resonant factor for torsional effect $R_{eff,t}$, while New Eurocode G (Eurocode 1-4, 2024) uses logarithmic decrement, resulting in different expressions for $R_{eff,t}$. However, given the conversion relationship between logarithmic decrement and damping ratio, the calculation procedures in both codes/standards are fundamentally equivalent.

$$\hat{\theta}_{max} = \frac{0.6g_r \frac{1}{2} \rho \overline{V}_z^2 hb^2 C_{f,t} R_{eff,t} K_t}{m_{1,t}} \quad (15)$$

3.4. Wind-induced lateral deflection/displacement

Among the codes and standards reviewed, Eurocode 1–4 (Eurocode 1-4, 2010), new draft of Eurocode 1–4 (Eurocode 1-4, 2024), AIJ (2004) (AIJ-RLB, 2004), NBCC (NBCC-Guidelines, 2017), and AS/NZS 1170.2 (AS/NZS 1170.2, 2021) do not provide a direct formula for calculating the maximum wind-induced displacement in the along-wind direction. Instead, they specify that the along-wind force equations provided in their respective codes/standards should be used to determine the maximum wind load. Following this, structural analysis should be performed to obtain maximum along-wind displacement. Consequently, verifying deflection criteria for in high-rise timber buildings becomes cumbersome.

Only ASCE 7–22 (ASCE/SEI 7-22, 2022) explicitly provides a direct formula for calculating maximum along-wind displacement, which is

Table 6
Summary of applicable conditions for the equations computing wind-induced torsional acceleration of building from codes and standards.

Code	AIJ (AIJ-Guidelines, 2004)	New Eurocode G (Eurocode 1-4, 2024)
Building shape	Rectangular cross-section	Rectangular cross-section
Dimensions	$h/\sqrt{bd} \leq 6$ and $0.2 \leq d/b \leq 5$ and $\frac{\overline{V}_z}{n_{1,t}\sqrt{bd}} = V_T \leq 10$ see note	$3 \leq h/\sqrt{bd} < 6$ and $0.2 \leq d/b \leq 5$ and $\overline{V}_z / (n_{1,t}\sqrt{bd}) = V_T \leq 10$ see note

Note: b is width of the building (horizontal dimensions perpendicular to the wind), d is depth of the building (horizontal dimension parallel to the wind), h is the height of the building, \overline{V}_z is mean wind velocity at the reference height z , $n_{1,t}$ is the natural frequency of the first torsional mode, V_T is the normalized velocity for torsional acceleration calculation.

represented in Equation (16). In this formula, \hat{X}_{max} is the maximum along-wind displacement, and the newly introduced G represents the gust-effect factor. This gust-effect factor can be determined using Equation (17). For the interpretation and calculation of all other parameters and factors, please refer to the ASCE part in Table 2 and Table 3. Equation (16) accounts only for the fundamental along-wind mode. Whether higher-order along-wind modes should also be included in displacement estimates remains a question.

$$\hat{X}_{max} = \frac{\rho \overline{V}_z^2 bh C_{f,x} KG}{8m_{1,x} \pi^2 n_{1,x}^2} \quad (16)$$

$$G = 0.925 \frac{1 + 1.7I_z \sqrt{\frac{11.56}{1 + 0.63 \left(\frac{b+h}{z}\right)^{0.63}} + g_r^2 \left(\frac{R_{eff,x}}{1.7}\right)^2}}{1 + 5.78I_z} \quad (17)$$

Only Eurocode 1–4 (Eurocode 1-4, 2010) and the Newdraft of Eurocode 1–4 (Eurocode 1-4, 2024), provide formulas for the direct calculation of maximum displacement of buildings in the across-wind direction under certain conditions. Specifically, the informative Annex E of Eurocode 1–4 (Eurocode 1-4, 2010) outlines two calculation methods known as Eurocode E1 and Eurocode E2 (Eurocode 1-4, 2010), while the informative Annex H in the new draft Eurocode 1–4 (Eurocode 1-4, 2024) introduces a single method referred as New Eurocode H (Eurocode 1-4, 2024).

In these annexes, the displacement in the across-wind direction is defined as the across-wind amplitude of the structure caused by vortex-shedding activity. The specific application conditions for the three methods are summarized in Table 8. All annexes indicate that for structures with rectangular cross-sections, when the critical wind velocity V_{crit} , calculated by Equation (18), exceeds 1.25 times the mean wind velocity, vortex-shedding effects can be neglected. In this context, S_t denotes the Strouhal number, $n_{1,y}$ represents the natural frequency in the across-wind direction, and b is the building width perpendicular to the wind direction. Because tall timber buildings may have irregular shapes, as mentioned before, the available formulas for across-wind displacement may not apply, limiting their usefulness.

$$V_{crit} = \frac{bn_{1,y}}{S_t} \quad (18)$$

For structures with circular cross-sections, the critical wind velocity is taken to be half the value calculated by Equation (18). The calculation method provided in Eurocode E1 (Eurocode 1-4, 2010) is given by Equation (19), where \hat{y}_{max} is the maximal across-wind displacement, $K_{y,dis}$ is the mode shape factor for across-wind displacement, K_w is effective correlation length factor, C_{lat} is the lateral force coefficient, b is the building width perpendicular to the wind direction, S_c is the Scruton number and S_t is the Strouhal number.

$$\hat{y}_{max} = \frac{K_{y,dis} K_w C_{lat} b}{S_c S_t^2} \quad (19)$$

The formulas for Eurocode E2 (Eurocode 1-4, 2010) and New Eurocode H (Eurocode 1-4, 2024) are identical and are presented as Equation (20), where C_1 and C_2 are parameters further calculated by Equation (21) and (22) respectively. Additionally, $K_{p,ac}$ is the peak factor for across-wind displacement and can be computed by using Equation (23). It is important to note that Equation (20) also appears in the AS/NZS (AS/NZS 1170.2, 2021) standard. However, this formula is explicitly designated for calculating the maximum tip deflection amplitude of chimneys, masts, or poles with circular cross-sections (excluding attachments such as ladders or strakes near the top) subjected to crosswind vibrations caused by vortex shedding at critical wind speed. As it is not intended for building applications, this method in AS/NZS is excluded from the present discussion. The values and

Table 7

Summary of values and calculation methods for the parameters in the equations computing wind-induced torsional acceleration of building from codes and standards.

	$C_{f,t}$	$R_{off,y}$	K_t	$m_{1,t}$	$\phi_{1,t}(z)$
AIJ (AIJ-Guidelines, 2004)	$\left[0.0066 + 0.015 \left(\frac{d}{b}\right)^2\right]^{0.78}$	$\sqrt{\frac{\pi F_t}{4\beta_t}}$	$1 - 0.4 \ln \xi$	$\int_0^h i(z)\phi_{1,t}^2(z)dz$	$(z/h)^\xi$
New Eurocode G (Eurocode 1-4, 2024)	$\left[0.0066 + 0.015 \left(\frac{d}{b}\right)^2\right]^{0.78}$	$\sqrt{\frac{\pi^2 F_t}{2\delta_{t,s}}}$	1	$\int_0^h i(z)\phi_{1,t}^2(z)dz$	z/h

Note.
 β_t : the damping ratio in the torsional direction.
 $\delta_{t,s}$: the logarithmic decrement of structural damping in torsional direction. No specific value is listed for timber buildings. However, for timber bridges, a range of 0.06–0.12 is indicated.

$$F_t = \begin{cases} \frac{0.14K_T^2 V_T^{2\beta} d(b^2 + d^2)^2}{\pi^2 b^3}, & (V_T \leq 4.5 \text{ or } 6 \leq V_T \leq 10) \\ F_{4.5} \exp\left[3.5 \ln\left(\frac{F_6}{F_{4.5}}\right) \ln\left(\frac{V_T}{4.5}\right)\right], & (4.5 < V_T < 6) \end{cases}, \quad l = \begin{cases} b, & (b \geq d) \\ d, & (b < d) \end{cases}, \quad F_{4.5} = F_t|_{V_T=4.5}, \quad F_6 = F_t|_{V_T=6}, \quad K_T =$$

$$\beta = \begin{cases} \frac{-1.1(d/b) + 0.97}{(d/b)^2 + 0.85(d/b) + 3.3} + 0.17, & (V_T \leq 4.5) \\ \frac{0.077(d/b) - 0.16}{(d/b)^2 - 0.96(d/b) + 0.42} + \frac{0.35}{(d/b)} + 0.095, & (6 \leq V_T \leq 10) \end{cases};$$

ξ : mode shape exponential coefficient for the mode shape in torsional direction $\phi_{1,t}(z) = \left(\frac{z}{h}\right)^\xi$;

V_T : the normalized velocity for torsional acceleration calculation, see Table 6.

$i(z) = \mu(z)(b^2 + d^2)/12$, where $\mu(z)$ is the mass per unit height at height z .

calculation formulas for the above parameters are provided in Table 9.

$$\hat{Y}_{max} = bK_{p,ac} \sqrt{C_1 + \sqrt{C_1^2 + C_2}} \quad (20)$$

$$C_1 = \frac{a_L^2}{2} \left(1 - \frac{S_c}{4\pi K_a}\right) \quad (21)$$

$$C_2 = \frac{\rho b^2 a_L^2 C_c^2 i}{m_{1,y} K_a S_a^4 h} \quad (22)$$

$$K_{p,ac} = \sqrt{2} \left\{1 + 1.2 \arctan \left[0.75 \left(\frac{S_c}{4\pi K_a}\right)^4\right]\right\} \quad (23)$$

The New draft of Eurocode 1–4 (Eurocode 1-4, 2024) has removed the original Eurocode E1 (Eurocode 1-4, 2010) method found in the previous version. While the New Eurocode H method is similar to Eurocode E2 and does not impose dimensional requirements initially, several dimensional constraints arise when calculating or selecting parameters, such as S_t , a_L , C_c and K_a within its formulas. Most of these constraints are dependent on the building’s aspect ratio (d/b). Consequently, designers may overlook the applicability and limitations of the code procedures at the outset, leading to misapplication and unnecessary complications in the design process.

Notably, when the aspect ratio (d/b) falls between 1.5 and 2.5, selecting parameter values (S_t , a_L , C_c and K_a) become uncertain or values are not provided at all. Unfortunately, the aspect ratios of existing high-rise timber structures may fall within this range; for instance, the Mjöstårnet building has an aspect ratio of approximately 2 (Abrahamsen, 2017). This suggests that the displacement calculation formula for across-wind response in the new Eurocode draft (Eurocode 1-4, 2024) may not be entirely applicable to modern high-rise timber buildings. Furthermore, none of the reviewed codes or standards provide formulas that address both across-wind and along-wind displacement simultaneously, which complicates the calculation of maximum overall displacement.

3.5. Combination methods of wind effects

In practice, wind-induced responses, accelerations and displacements in the along-wind, across-wind, torsional, and even vertical directions, occur simultaneously rather than in isolation. An accurate comfort assessment therefore requires combining the peak effects from all relevant directions, as the resultant response is usually greater than any individual component.

Table 10 provides an overview of direct calculation methods and combination approaches for assessing wind effects as outlined in the reviewed codes and standards. Only three (AS/NZS (AS/NZS 1170.2, 2021), AIJ (AIJ-RLB, 2004), and the new draft Eurocode 1–4 (Eurocode

Table 8

Summary of applicable conditions for the procedure computing wind-induced across-wind displacement of building from codes and standards.

Code	Eurocode E1 (Eurocode 1-4, 2010)	Eurocode E2 (Eurocode 1-4, 2010)	New Eurocode H (Eurocode 1-4, 2024)
Suitable scenarios	This approach applies to various structural types and mode shapes, incorporating turbulence and roughness effects. It is suitable for use under normal climatic conditions.	This approach applies to buildings with a regular across-wind dimension distribution along the main axis. It is not suitable for grouped or in-line arrangements or coupled cylinders. The method accounts for varying turbulence intensities influenced by meteorological conditions. Additionally, it can be applied in regions prone to extremely cold and stratified flow conditions.	
Dimensional requirements	$0.5 \leq d/b \leq 10$ see note *1	–	Same as it in Table 4

Note: b is width of the building (horizontal dimensions perpendicular to the wind), d is depth of the building (horizontal dimension parallel to the wind), h is the height of the building.

*1: This dimensional requirement is for a building with rectangular cross-section.

Table 9

Summary of values and calculation methods for parameters in the equations computing wind-induced across-wind displacement of building from codes and standards.

Parameters	K_w	$K_{y,dis}$	C_{lat}	S_c	S_i	
Eurocode E1 (Eurocode 1-4, 2010)	$\frac{3L_j}{h} - \frac{3L_j^2}{h^2} + \frac{L_j^3}{h^3}$ see note ¹	0.13 see note ²	$\begin{cases} C_{lat,0}, \text{ when } \frac{V_{crit}}{V_{m,L}} \leq 0.83 \\ C_{lat,0} \left(3 - 2.4 \frac{V_{crit}}{V_{m,L}} \right), \text{ when } 0.83 \leq \frac{V_{crit}}{V_{m,L}} < 1.25 \\ 0, \text{ when } 1.25 < \frac{V_{crit}}{V_{m,L}} \end{cases}$	$\frac{2\delta_{y,s}m_{1,y}}{\rho b^2}$	see note ⁴	
Parameters	a_L	C_c	i	$m_{1,y}$	K_a	S_c
Eurocode E2 (Eurocode 1-4, 2010)	0.4	Provided as tables, see note ⁵	b	$\int_0^h \mu(z)\phi_{1,y}^2(z)dz$	$K_{a,max}$ see note ⁷	$\frac{2\delta_{y,s}m_{1,y}}{\rho b^2}$
New Eurocode H (Eurocode 1-4, 2024)	Provided as tables, see note ⁸	Provided as tables, see note ⁹	d	$\int_0^h \phi_{1,y}^2(z)dz$ or approximation ⁶	$K_{a,max}h(I_u)$ see note ¹⁰	$\frac{2\delta_{y,s}m_{1,y}}{\rho b d}$

Note: b is width of the building (horizontal dimensions perpendicular to the wind), d is depth of the building (horizontal dimension parallel to the wind), h is the height of the building. As defined, i equals to b in the Eurocode E2 and i equals to d in the new Eurocode H, respectively.

*1: It is assumed that the ξ (see Note of Table 5) is equal to 2. L_j is the correlation length, no explicit definition is provided in the code. The correlation length is expressed as a function of maximum horizontal displacement of a structure in the vibration, which should be positioned in the region of antinodes. The value of L_j should be taken as $6b$ when $\hat{y}_{max}/b < 0.1$, a condition typically met by most buildings. However, for timber structures, $6b$ may be larger than the building height itself.

*2: It is assumed that the ξ (see Note of Table 5) is equal to 2.

*3: V_{crit} should be calculated using Equation (18). Here, $V_{m,L}$ is the mean wind velocity in the central of correlation length (see note 1), $C_{lat,0}$ is the basic value of lateral force coefficient, provided in the tabular and graphical form. For building with rectangular cross-section, $C_{lat,0} = 1.1$. For building with circular cross-section, the value of $C_{lat,0}$ depends on the Reynolds number.

*4: The Strouhal number is provided in tabular and graphical formats. In the Eurocode 1–4, for buildings with circular cross-sections, a value of 0.18 is recommended. For rectangular cross-sections, the Strouhal number is given as a curve dependent on the value of d/b . On the other hand, in the new draft of Eurocode 1–4, the Strouhal number is not constant. For circular buildings, it depends on the Reynolds number, while for rectangular buildings, it is related to the d/b ratio. The new draft of the European standard highlights that when $d/b < 3.5$, the Strouhal number is influenced by multiple factors (e.g., turbulence, vibration amplitudes, Reynolds number), and when $1.5 < d/b < 2.5$, its value becomes highly uncertain.

*5: The value is provided in tabular form: for square cross-section structures, the C_c is 0.04; for circular cylinders, it varies with the Reynolds number and can be determined through linearly interpolation with the logarithm Reynolds number.

*6: For cantilevered structures (e.g., buildings) with varying mass distributions, it can be approximated by the average mass of the upper third of the structure.

*7: The parameter K_a decreases as turbulence intensity increases. $K_{a,max}$ represents the value of K_a when turbulence intensity is zero. Using $K_a = K_{a,max}$ under non-zero turbulence conditions yields conservative displacement predictions. More details can be found in the national annex. The values of $K_{a,max}$ are provided in tabular form: for square cross-section structures, the $K_{a,max}$ is 0.04; for circular cylinders, it varies with the Reynolds number and can be determined through logarithm interpolation.

*8: The value is provided in tabular form: for circular cylinders, a_L is 0.4; For rectangular building, $a_L = \begin{cases} 0.6, \text{ when } 0.25 \leq d/b \leq 1.25 \\ 0.1, \text{ when } 3 \leq d/b \leq 5 \end{cases}$, the interpolation is not allowed.

*9: Additional guidance could be given in the national annex for the value of C_c . In the New draft Eurocode 1–4, the maximal value of C_c (i.e., $C_{c,max}$) is suggested. $C_{c,max}$ is provided in tabular form: for circular cylinders, it varies with the Reynolds number (e.g., when Reynolds number is equal to or less than 100000, the $C_{c,max}$ is equal to 0.01) and can be determined through linearly interpolation with the logarithm Reynolds number; For rectangular building, $C_{c,max} = \begin{cases} 0.03, \text{ when } 0.25 \leq d/b \leq 1.25 \\ 0.03, \text{ when } 3 \leq d/b \leq 5 \end{cases}$, the interpolation is not allowed.

*10: The value of $K_{a,max}$ is provided in tabular form: for circular cylinders, it varies with the Reynolds number and can be determined through logarithm interpolation; For rectangular building, $K_{a,max} = \begin{cases} 6, 0.25 \leq d/b \leq 1.25 \\ 3, 3 \leq d/b \leq 5 \end{cases}$, the interpolation is not allowed. $h(I_u) = \begin{cases} 1 - 3I_u, 0 \leq I_u \leq 0.25 \\ 0.25, 0.25 \leq I_u \end{cases}$, where I_u is the turbulence intensity at the height where it has the largest movement.

Table 10

Summary of availability of calculation procedure for wind-induced vibration effects from codes and standards.

Codes/Standards	Along-wind effects		Across-wind effects		Torsional effects		Combination effects
	Acc.	Disp.	Acc.	Disp.	Acc.	Disp.	
ASCE 7–22 (ASCE/SEI 7-22, 2022)	Yes	Yes	No	No	No	No	No
NBCC (NBCC-Guidelines, 2017; NBCC, 2018)	Yes	No	Yes	No	No	No	No
Eurocode 1–4 (Eurocode 1-4, 2010)	Yes	No	No	Yes	No	No	No
AS/NZS 1170.2 (AS/NZS 1170.2, 2021)	Yes	No	Yes	No	Yes	Yes	Yes
AIJ (AIJ-RLB, 2004)	Yes	No	Yes	No	Yes	No	Yes
New draft Eurocode 1–4 (Eurocode 1-4, 2024)	Yes	No	Yes	Yes	Yes	No	Yes

Note: Acc. represents acceleration; Disp. represents displacement. Yes indicates that the code/standard provides a direct method for calculating the corresponding effect; No indicates that it does not provide a direct method.

1-4, 2024)) offer direct and comprehensive methods for calculating overall (omnidirectional) wind-induced acceleration. However, none of these standards provide a complete and direct method for calculating

overall wind-induced displacement.

Among the reviewed codes and standards, ASCE 7–22 (ASCE/SEI 7-22, 2022), NBCC (NBCC-Guidelines, 2017; NBCC, 2018), and

Eurocode 1–4 (Eurocode 1-4, 2010) do not provide combined calculation methods for wind-induced acceleration or displacement. However, both ASCE 7–22 (ASCE/SEI 7-22, 2022) and NBCC (NBCC-Guidelines, 2017; NBCC, 2018) offer procedures for combining wind loads in three directions: along-wind, across-wind, and torsional. Through additional structural analysis, these procedures can theoretically be utilized to determine the maximum wind-induced displacement.

The appendix of AS/NZS 1170.2 (AS/NZS 1170.2, 2021) introduces formula (24) to combine peak accelerations in different directions, offering a comprehensive evaluation. In this formula, $a_{(x,y,z)}$ represents the overall peak acceleration, while \hat{x}^2 , \hat{y}^2 and \hat{z}^2 are the peak acceleration components of a structure along the x-axis (along-wind direction), y-axis (across-wind direction), and about z-axis (torsional direction), respectively. The ratio ρ_c indicates the relationship between the peak acceleration of the largest component and that of the second-largest component (therefore with a value greater than 1). This formula is applicable in scenarios where the three acceleration components are generally not significantly coupled.

$$a_{(x,y,z)} = \frac{\rho_c}{\sqrt{1 + \rho_c^2}} \times \sqrt{\hat{x}^2 + \hat{y}^2 + \hat{z}^2} \tag{24}$$

The AIJ (AIJ-RLB, 2004) and the New draft Eurocode 1–4 (Eurocode 1-4, 2024) provide similar wind effect combination methods, outlining three combination cases, as summarized in Table 11. In Combination case 1, the along-wind effect is treated as the dominant factor, with the across-wind and torsional effects included using a reduction factor of 0.4. Combination cases 2 and 3 consider the across-wind and torsional effects as the dominant factors, respectively. In these cases, the along-wind effect is integrated with a reduction factor that depends on the along-wind gust effect factor G_D , and a combination factor γ_{LT} (its value is shown in Table 12) is applied to the remaining across-wind or torsional effects.

3.6. Estimation of damping and natural frequency

As outlined in the preceding review of wind-induced response formulas, most of these formulas require the structural natural frequency and damping ratio/logarithmic decrement of damping as inputs. Typically, the natural frequency must be derived through detailed modelling and modal analysis, while damping ratios are often adopted from literature. To enable rapid assessment of wind-induced responses in timber buildings, this section studies methods for estimating natural frequencies and presents recommended damping values from various codes and standards. A summary of relevant approaches and values might be applicable to timber structures is provided in Table 13. A detailed discussion of each standard follows:

Table 11
Combination rules for wind-induced effects from different wind directions.

Combination	Along-wind effects	Across-wind effects	Torsional effects
1	D	$0.4L$	$0.4T_t$
2	$D \left(0.4 + \frac{0.6}{G_D} \right)$	L	$\gamma_{LT} T_t$
3	$D \left(0.4 + \frac{0.6}{G_D} \right)$	$\gamma_{LT} L$	T_t

Note: D is along-wind effects; L is across-wind effects; T_t is torsional effects; G_D is the along-wind gust factor, AIJ (AIJ-RLB, 2004) and New draft Eurocode 1–4 (Eurocode 1-4, 2024) provide different formulas for calculating G_D . Due to the length and complexity of these formulas and their parameter calculations, they are not detailed here. For further information, refer to Section F.5.4 of Annex F in New draft Eurocode 1–4 (Eurocode 1-4, 2024) and Section A6.3.1 of AIJ (AIJ-RLB, 2004). γ_{LT} is the combination coefficient, its value is shown in Table 12.

Table 12
The value of the combination coefficient γ_{LT}

d/b	$n_{1,yt}/\bar{V}_z$	γ_{LT}		
		$f_{LT} = 1.0$	$f_{LT} = 1.1$	$f_{LT} \geq 1.4$
≤ 0.5	≤ 0.1	0.95	0.61	0.55
	0.2	0.55	0.67	0.61
	0.3	0.55	0.73	0.67
	0.6	0.79	0.79	0.79
	≥ 1	0.84	0.84	0.84
1	≤ 0.1	0.84	0.55	0.55
	0.2	0.61	0.55	0.55
	0.3	0.55	0.55	0.55
	0.6	0.67	0.67	0.67
	≥ 1	0.73	0.73	0.73
≥ 2	≤ 0.05	0.79	0.55	0.55
	≥ 0.1	0.55	0.55	0.55

Note: b is width of the building (horizontal dimensions perpendicular to the wind); d is depth of the building (horizontal dimension parallel to the wind); \bar{V}_z is the mean wind velocity at evaluation height z .

$$n_{1,yt} = \begin{cases} n_{1,y}, n_{1,y} < n_{1,t}, & \text{where, } n_{1,y} \text{ and } n_{1,t} \text{ are the natural frequency of the} \\ n_{1,t}, n_{1,y} \geq n_{1,t}, & \end{cases}$$

first mode in across-wind and torsional direction, respectively; $f_{LT} =$

$$\begin{cases} n_{1,t}/n_{1,y}, n_{1,y} < n_{1,t}, \\ n_{1,y}/n_{1,t}, n_{1,y} \geq n_{1,t}, \end{cases} \text{ Linear interpolation is allowed.}$$

- ASCE: In the main body of ASCE 7–22 (ASCE/SEI 7-22, 2022), Section 26.11 provides four formulas for estimating the lower-bound natural frequency of concrete or structural steel buildings with various lateral systems. However, there is no formula given for approximating the natural frequency of timber buildings. In the commentary to Section C26.11, several formulas are referenced for the general estimation of building natural frequencies. Among these, three formulas depend solely on building height. While one formula (marked with * in Table 13), intended for cantilevered masts or poles with uniform cross-sections, incorporates bending stiffness and mass per unit height, whether it is applicable for timber buildings or not, which should be further investigated. Additionally, the commentary suggests damping ratios of 1% and 2% for steel and concrete buildings, respectively, which were typically used in the U.S. But the commentary sector of the code does not provide recommendations of damping ratios for timber buildings.
- NBCC: The NBCC (the standard) and NBCC-Guideline (NBCC-Guidelines, 2017; NBCC, 2018) do not provide a specific method for estimating a building’s natural frequency. However, Section 4.1.7.8 of the NBCC (the standard) (NBCC, 2018) (Dynamic Procedure) specifies the following nominal damping ratios: 1% for steel structures, 2% for concrete structures, and 1.5% for composite structures. The accompanying NBCC-Guideline (NBCC-Guidelines, 2017) clarifies that “composite structures” are those in which both steel and concrete contribute to lateral load resistance. No explicit recommendations are given for timber buildings. The NBCC-Guideline (NBCC-Guidelines, 2017) suggests estimating natural frequency of a building via finite element analysis or Rayleigh’s method (NBCC-Guidelines, 2017; NBCC, 2018), which requires the associated wind force on floor (F_i) and deflection (x_i) obtained from static analysis. However, due to the complexity of acquiring these parameters, this method may not be practical for quick estimations of natural frequencies.
- AIJ: The AIJ-RBL (AIJ-RLB, 2004) standard does not provide estimation methods or recommended values for the natural frequencies or damping ratios of buildings. In Japan, the damping ratio and natural frequency of buildings are typically estimated using empirical formulas proposed by Tamura (2003). These formulas relate natural frequency to building height, while the damping ratio

Table 13

Estimated values and methods for natural frequencies and damping ratios might be applicable to timber buildings, as provided in codes/standards.

Codes/standards	Natural frequency (Hz) n_1	Damping ratio β /Logarithmic decrement δ
ASCE (ASCE/SEI 7-22, 2022)	$n_1 = 100/H$ (ft) average value ($H < 400$ ft); $n_1 = 75/H$ (ft) lower bound value ($H < 400$ ft); $n_1 = 150/H$ (ft) (more accurate for $H > 400$ ft); $n_1 = (0.56/h^2) \sqrt{EI/\mu}$ uniform cross-section (*)	-
NBCC (NBCC-Guidelines, 2017; NBCC, 2018)	$n_1 = \frac{1}{2\pi} \sqrt{\frac{\sum_{i=1}^N F_i \frac{x_i}{x_N}}{x_N \sum_{i=1}^N M_i \left(\frac{x_i}{x_N}\right)^2}}$ (Rayleigh's method)	-
AIJ (AIJ-Guidelines, 2004)	-	-
AS/NZS (AS/NZS 1170.2, 2021)	-	-
Eurocode 1-4 (Eurocode 1-4, 2010)	$n_1 = 46/h$ ($h > 50$ m)	$\delta = \delta_s + \delta_a + \delta_d$
New draft Eurocode 1-4 (Eurocode 1-4, 2024)	$n_1 = 46/h$ ($h > 50$ m); (for reinforced concrete, composite and steel buildings); $n_{1,t} = 1.3n_1$ $n_1 = \frac{1}{2\pi} \sqrt{\frac{3EI_b}{M_s h^3}}$ (for buildings with uniformly distributed stiffness and mass); $n_i = \frac{K_i}{2\pi} \sqrt{\frac{EI}{\mu h^4}}$ (for cantilever-like buildings with uniformly distributed stiffness and mass)	$\delta = \delta_s + \delta_a + \delta_d$

Note: n_1 is the natural frequency of the first mode in flexural. H is the height of the building in foot; h is the height of the building in meter; E is the modulus of elasticity. I is the second moment of the cross-section. μ is mass per unit height. N is the total number of floors; F_i is the associated wind force on floor i , resulting in the horizontal deflection x_i , which could be determined by structural analysis; M_i is the associated mass of floor i . $n_{1,t}$ is the frequency of the first mode in torsional direction. I_b is the moment of inertia of the cross-section. M_s is the equivalent mass, $M_s = m_c + \mu h/4$, where m_c is concentrated mass. n_i is i -th

bending frequency. $K_i = \begin{cases} 3.52 & i = 1 \\ 22 & i = 2 \\ 61.7 & i = 3 \end{cases}$. δ_s is the logarithmic decrement of

structural damping, δ_a is the logarithmic decrement of aerodynamic damping for the fundamental mode and δ_d is the logarithmic decrement of damping due to special devices. The following formula is given to estimate the δ_a for buildings:

$$\delta_a = \begin{cases} \frac{\rho \bar{V}_z^2 b C_{f,x}}{2m_{1,x} n_{1,x}} & \text{along - wind} \\ \frac{\rho \bar{V}_z^2 d C_{f,y}}{4m_{1,y} n_{1,y}} & \text{across - wind} \end{cases}, \text{ the explanation and calculation of parameters}$$

please see Tables 2 and 5; Approximate values for δ_s are provided in tabular form according to structural type. No specific value is listed for timber buildings. However, for timber bridges, a range of 0.06–0.12 is indicated.

depends on frequency and amplitude of vibrations. However, these formulas apply only to steel and reinforced concrete structures, with no specific provisions for timber buildings.

- AS/NZS: The code/standard (AS/NZS 1170.2, 2021) does not provide a method for estimating building frequency. However, Section 6.4 (Along-wind response) recommends three damping ratio values for steel and reinforced concrete structures. The highest damping ratio range (e.g., 1.5% - 2.0% for steel structure and 2.0% - 3.0% for reinforced concrete structures) is recommended for ultimate limit state (ULS) design, the intermediate damping ratio range (e.g., 1.0%

- 1.2% for steel structure and 1.0% - 1.5% for reinforced concrete structures) is suggested for deflection-based serviceability limit state (SLS) design, and the lowest (e.g., 0.5% - 1.0% for steel structure and 0.8% - 1.2% for reinforced concrete structures) is for acceleration-based SLS design. While no damping ratios are specified for timber buildings, the idea of tailoring recommendations based on different design states is noteworthy.

- Eurocode 1-4 and the New draft Eurocode 1-4: Eurocode 1-4 (Eurocode 1-4, 2010) provides a simple empirical formula for estimating the natural frequency of a building, linearly related to the inverse of its height. This approximation is coarse, as it disregards structural type and material. The new draft of Eurocode 1-4 (Eurocode 1-4, 2024) improves upon this by introducing an estimation for the first rotational mode frequency, which is calculated as 1.3 times that of the fundamental deflection mode frequency. Additionally, it offers formulas for estimating the first three flexural frequencies of cantilever structures that have uniformly distributed mass and stiffness, taking into consideration factors like material modulus, moment of inertia, and mass. These enhancements may be particularly beneficial for timber buildings, which should be further validated. Both Eurocode 1-4 (2010) and new draft Eurocode 1-4 (2024) express structural damping using the logarithmic decrement rather than the damping ratio. They define total damping as consisting of three components: structural damping (from internal friction), aerodynamic damping (from fluid-structure interaction), and supplemental damping devices. Eurocode 1-4 (2010) provides formulas for calculating aerodynamic damping in the along-wind direction, which are retained in the new draft (2024), along with additional formulas introduced for across-wind damping. Although both versions include estimates for structural damping across various structural types, timber building types are not specifically addressed. However, for timber bridges, a suggested logarithmic decrement range of 6%–12% may serve as a reference for timber buildings. The damping range reported for timber bridges is believed to be relevant for timber-building design, one opinion is that the conceptual structure of Mjøstårnet (as one of the highest timber buildings) is comparable to a vertical standing glulam truss bridge, as stated in the study by Tulebekova et al. (2024). According to Tulebekova et al. (2024), this analogy motivated the use of a 1.9% damping ratio in the wind-induced-vibration design of Mjøstårnet, although this rationale is not stated in the paper (Abrahamsen, 2017) published by the Mjøstårnet design team.

This section reviews the procedures outlined in various codes and standards for computing wind-induced accelerations and lateral deformation, along with the prescribed methods for combining along-wind, across-wind, and torsional effects. To facilitate rapid preliminary checks, the section also summarizes provisions related to frequency and damping estimation contained in these documents. The review revealed that:






- None of the reviewed codes or standards supplies a complete set of calculation procedures for all six wind-induced vibration effect components, three directions (along-, across- and torsional directions) and two response types (accelerations and deflections), and their combinations.
- All available methods for assessing wind-induced accelerations and most procedures for computing wind-induced lateral deflections, restrict the analysis to the fundamental vibration mode. Neglecting higher-order modes can result in systematic underestimation of wind-induced responses.
- Many wind-vibration procedures impose geometric constraints - such as specifying a rectangular plan, a particular slenderness ratio, or a narrow aspect-ratio range - that modern high-rise timber buildings may not fulfill. When these conditions are not met, the codified formulas cannot be applied directly, and designers must

resort to supplemental tools such as computational fluid-dynamics simulations (CFD) or wind-tunnel tests to complete the wind-induced vibration assessment.

- The quick-estimation formulas for natural frequency and the damping recommendations in current codes and standards are calibrated almost exclusively for concrete or steel structures. Correlations for

timber buildings are largely lacking, particularly with respect to reliable damping ranges. A comprehensive statistical survey of measured damping ratios in timber buildings, followed by the development of empirical relationships or recommended value range is therefore strongly encouraged.

Table 14
Design cases of high-rise timber building against wind-induced vibration.

Building	Ascent	Mjøstårnet	Haut	Brock Commons	Fyrtnorget
Schematic of the structure (Sources: (Abrahamsen, 2017; Fernandez et al., 2020; Laurent et al., 2023; Verhaegh et al., 2020; Poirier et al., 2016))					
Country	United States	Norway	Netherlands	Canada	Sweden
Height [m]	86.6	85.4	73.0	54.8	51.0
Structural system	Concrete podium + Concrete cores + Timber columns and beams + CLT floors	Timber posts and beams + Timber braces + Timber floors and concrete floors (see note 1)	Concrete podium + Concrete core + CLT shear walls + timber beams + steel and concrete edge beams + TCC floors	Concrete podium + Concrete core + Timber posts and beams + CLT floors	Timber posts and beams + CLT core + diagonals + CLT floors
Considered effects	Not mentioned	Along-wind acceleration (see note 2)	Along-wind and across-wind acceleration (see note 3)	Along-wind and across-wind acceleration (see note 3)	Along-wind, across-wind, torsional acceleration and their combination
Criteria	Not mentioned	ISO 10137 (ISO 10137, 2007)	Dutch annex of Eurocode (1990) (National Annex to NEN, 2011)	NBCC (NBCC-Guidelines, 2017; NBCC, 2018)	ISO 10137 (ISO 10137, 2007)
Calculation method	Not mentioned	Eurocode 1–4 (Eurocode 1-4, 2010)	NBCC (NBCC-Guidelines, 2017; NBCC, 2018)	NBCC (NBCC-Guidelines, 2017; NBCC, 2018)	Eurocode 1–4 (Eurocode 1-4, 2010) + NBCC (NBCC-Guidelines, 2017; NBCC, 2018) + Extra reference (Konrad and Johann-Dietrich, 2003) + Wind tunnel test
Damping design	Not mentioned	Damping ratio of 1.9%	Structural Damping ratio of 1.5%	Damping ratio of 1.5%	Logarithmic damping decrement 0.12 (equal to damping ratio 1.9%)
Design value of natural frequency (see note 4)	Not mentioned	$n_{1,x} = 0.33 \text{ Hz}$ $n_{1,y} = 0.37 \text{ Hz}$	$n_{1,x} = 0.43 \text{ Hz}$ $n_{1,y} = 0.53 \text{ Hz}$ $n_{1,t} = 0.57 \text{ Hz}$	$n_{1,x} = 0.5 \text{ Hz}$	$n_{1,x} = 0.72 \text{ Hz}$ $n_{1,y} = 0.73 \text{ Hz}$ $n_{1,t} = 0.97 \text{ Hz}$
Design value of wind-induced acceleration	Not mentioned	Around 0.068 m/s^2 (1-year return period)	10 mg (around 0.098 m/s^2) (1-year return period)	1.5 \% g (around 0.147 m/s^2) (10-year return period)	2.4 \% g (around 0.235 m/s^2) (10-year return period) and 0.7 \% g (around 0.069 m/s^2) (1-year return period)
Remarkable points	<ul style="list-style-type: none"> • Wind loading governed the design of the lateral system. • The lateral load was designed to be transferred to the concrete cores through timber floor panels, wood splines, and steel strapping functioned. 	<ul style="list-style-type: none"> • Additional mass was introduced in the upper third of the building (12th to 18th floors) by replacing timber floors with concrete to meet comfort criteria. • According to the design, while acceleration at Level 17 complies with the comfort criteria, that of Level 18 slightly exceeds it. The client has accepted this condition. 	<ul style="list-style-type: none"> • Lateral stability and torsional effects are ensured by a concrete core and two CLT shear walls. • Due to the lack of experience, it was decided to utilize the CLT walls only for SLS. The concrete core was designed to carry the full wind loads under ULS. • Wind response of the building is highly mass-dependent, supporting the design decision of the heavier concrete core and TCC floor. 	<ul style="list-style-type: none"> • All connections were carefully designed, and drag straps were employed to enable the CLT floor panels to function as diaphragms, transferring lateral loads from all directions to the cores. • Accelerometers were installed at both the top and ground levels to monitor acceleration in both principal directions of the building. 	<ul style="list-style-type: none"> • Sensitivity analysis indicated that 20% variation in connection stiffness values and stiffness of the bracing elements did not affect acceleration significantly. • Along-, across-wind, torsional accelerations and combination, were examined. Due to inherent uncertainties and the absence of guidance, additional wind tunnel tests were conducted.

Note.
 1: Floors 2 to 11 are prefabricated timber decks, while floors 12 to 18 are concrete floors (cast in-situ of upper part).
 2: Along-wind accelerations were examined in both directions.
 3: The examination of across-wind acceleration was not clearly mentioned. Since the method of NBCC (NBCC-Guidelines, 2017) was used, it is speculated that an across-wind acceleration was analyzed.
 4: For details on the specific vibration modes and corresponding directions of the listed natural frequencies, please refer to the original data source (Abrahamsen, 2017; Laurent et al., 2023; Michele et al., 2023; Canadian Wood Council, 2018).

4. Design cases of high-rise timber buildings

This section studies selected high-rise timber buildings with a focus on their wind-induced vibration design strategies. Publicly available information on detailed wind design is limited, as such data usually remains within the design teams. Therefore, this study is based on a small number of publications from those teams. Ultimately, five buildings were selected for analysis: Ascent (Fernandez et al., 2020), Mjøstårnet (Liven and Abrahamsen, 2023), Haut (Verhaegh et al., 2020), Brock Commons (Poirier et al., 2016) and Fyrtornet building (Laurent et al., 2023). According to the Council on Tall Buildings and Urban Habitat (Council on Tall Buildings and Urban Habitat, 2022) rankings as of this writing, these buildings are recognized as the world's tallest timber structures: Ascent is ranked 1st, Mjøstårnet 2nd, Haut 4th, and Brock Commons 12th. One recently completed building, although not yet listed in the ranking, stands less than 7 m shorter than Brock Commons building and was included due to the comprehensive wind design documentation available in the literature. Table 14 summarizes the general data and wind-resistance design approaches for each building, followed by a detailed discussion of each case.

4.1. Ascent

Ascent is a 25-storey (86.6 m) residential tower in Milwaukee, USA, currently recognized as the world's tallest timber building (Council on Tall Buildings and Urban Habitat, 2022). The lower seven levels consist of a post-tensioned concrete podium (190 mm thick), functioning primarily as a parking structure (Fernandez et al., 2020). Above this podium, the gravity system comprises Austrian-spruce glulam columns and beams supporting one-way, 5-ply CLT floor panels (180 mm thick), with a 7-ply (240 mm) CLT panel used at the roof amenity deck. These elements are arranged on an efficient grid measuring 5.2 m × 6.1–7.6 m (Fernandez et al., 2020).

The lateral load-resisting system consists of reinforced-concrete core walls aligned with the vertical transportation shafts (Alejandro et al., 2024). The design of this lateral system was primarily influenced by wind loading, due to the building's proximity to Lake Michigan and the site's low seismicity. Lateral forces are transferred to the core walls at each level via diaphragms formed by the CLT panels, wood splines, and steel strapping. Although there is detailed documentation regarding fire protection and performance testing, public information on wind resistance design, natural frequency and vibration mitigation is limited (Fernandez et al., 2020).

4.2. Mjøstårnet

Mjøstårnet is an 18-storey mixed-use tower located on the shore of Lake Mjøsa in Brumunddal, Norway. The building features a rectangular plan measuring 16 × 37 m and is framed by four full-height glulam trusses with bracing, which provide both gravity and lateral resistance (Abrahamsen, 2018); Internal glulam beams and columns form the gravity frame, while the CLT elevator and stair shafts serve as secondary vertical elements that do not contribute to lateral stability. The highest occupied floor is located at 68.2 m (level 18), the architectural top reaches 85.4 m, and the lightning rod extends to 88.8 m (Abrahamsen, 2018).

Floors 2–11 employ lightweight timber cassette composite floors, while floors 12–18 use 300 mm concrete slabs (Abrahamsen, 2017); This hybrid system not only creates rigid diaphragms for efficient wind load transfer to the perimeter trusses but also increases mass in the upper 1/3 levels for vibration mitigation; The design was governed by wind loads rather than seismic effects. Wind-induced vibration calculations followed Eurocode 1–4 (Eurocode 1–4, 2010), assuming a structural damping ratio of 1.9% (inferred from the Treet tower in Bergen, Norway) and the natural frequency value obtained from modal analysis using FE software. The building's natural frequencies and peak

accelerations under 1-year return period of wind are illustrated in a figure where the x-axis represents frequency (Abrahamsen, 2017), though the exact values are not explicitly provided. According to Ascione et al. (2024), who obtained precise data through private communication with the design team, the fundamental natural frequencies of the modes in two translational direction are 0.33 Hz and 0.37 Hz, respectively (Ascione et al., 2024). Along-wind accelerations were evaluated under both long-side and short-side upwind conditions, respectively. The predicted roof drift was approximately 140 mm, and dynamic analyses showed that peak accelerations were within ISO 10137 (ISO 10137, 2007) comfort limits—borderline at level 17 and slightly above at level 18 (with the value of around 0.0068 m/s²), though these were deemed acceptable by the client. Due to the building's regular geometry and increased mass at the top, the design team considered wind tunnel testing and dampers to be unnecessary. (Liven and Abrahamsen, 2023).

4.3. Haut

Haut is a 21-storey residential building, standing 73 m tall, located on the Amstel River in Amsterdam, Netherlands (Verhaegh et al., 2020). The gravity system is hybrid: two CLT shear walls support timber-concrete-composite floors—160 mm CLT topped with 80 mm concrete. Perimeter glulam ring beams carry façade and balcony loads and serve as diaphragm ties. Cantilevering floors in the wedge-shaped north section are supported by steel- and concrete edge beams resting on two concrete columns. A two-storey concrete basement-plinth anchors the structure.

Lateral stability is provided by an eccentrically located in-situ concrete core in combination with two interior CLT shear walls to control torsional response (Verhaegh et al., 2020). Due to the limited precedents for this type of design, the concrete core was designed to resist full wind actions in ultimate limit states (ULS), while CLT walls were engaged only during serviceability limit states (SLS). Given the reduced mass of the structure compared to a conventional concrete frame, wind-induced vibration was a key design concern. Finite element modal analysis identified the fundamental vibration modes and corresponding natural frequencies: 0.43 Hz and 0.53 Hz for the two translational modes, and 0.57 Hz for the torsional mode (Michele et al., 2023). Assuming 1.5% structural damping (Verhaegh et al., 2020), peak top-floor accelerations under a one-year return wind (per NBCC method (NBCC-Guidelines, 2017; NBCC, 2018)) remained below 10 milli-g (Verhaegh et al., 2020), satisfying Dutch National Annex to Eurocode 1990 (National Annex to NEN, 2011) comfort limits. Sensitivity analysis confirmed the building's wind response is highly dependent on mass, thereby supporting the design decision to include a heavier concrete core and TCC floor system (Verhaegh et al., 2020).

4.4. Brock Commons

Brock Commons, located on the University of British Columbia campus in Vancouver, is an 18-storey residential tower that reaches a height of 54.8 m (58.5 m to the core parapet). The building provides 404 student beds across 15,000 m² of gross floor area (Poirier et al., 2016). Its gravity system is hybrid: featuring cast-in-place concrete foundations and a podium that supports a pair of 450 mm-thick reinforced-concrete elevator and stair cores that extend to the roof. These cores facilitate vertical circulation and provide lateral stiffness.

Levels 2–18 are framed with Austrian-spruce glulam (and some parallel strand lumber PSL) columns supporting 5-ply CLT floor panels topped with a thin concrete layer on a 4 m × 2.85 m grid. All lateral loads are resisted by the concrete cores. Each CLT diaphragm is supported by welded steel ledger angles and tied back using long drag-strap assemblies to ensure effective lateral load transfer to the cores and down to the raft foundations.

Compared to a concrete structure, the hybrid design of Brock

Commons is 7,648 t lighter, which reduces seismic inertia but increases sensitivity to overturning. Therefore, the cores were meticulously designed for both strength and stability. However, the design team did not disclose detailed information regarding wind load design (Poirier et al., 2016).

A report by the Canadian Wood Council (Canadian Wood Council, 2018) indicated that the Brock Commons building exhibited a first-mode frequency of 0.5 Hz: A dynamic wind load analysis was conducted using a finite-element model and the NBCC method (NBCC-Guidelines, 2017; NBCC, 2018), considering a 10-year return period for wind loading: The design aimed to limit wind-induced accelerations to 1.5 % of gravity at level 18, aligning with NBCC (NBCC-Guidelines, 2017; NBCC, 2018) recommendations for residential buildings, and a damping ratio of 1.5 % was assumed (Canadian Wood Council, 2018). Since the NBCC (NBCC-Guidelines, 2017; NBCC, 2018) provides procedures for both along-wind and across-wind acceleration calculations, it is inferred that both aspects were considered during the design process. To assess serviceability performance, permanent accelerometers were installed at the roof and ground levels to monitor horizontal vibrations during routine and extreme wind events (Poirier et al., 2016; Canadian Wood Council, 2018).

4.5. Fyrtornet

Fyrtornet is an 11-storey, 51 m-tall mass timber office tower located in the “Embassy of Sharing” development in Malmö, Sweden (Laurent et al., 2023). The gravity system consists of 5-ply CLT floor slabs that are 180 mm thick, with a 240 mm 7-ply slab at the library level and a concrete topping on the roof for added mass. These slabs span between a 280–320 mm thick CLT core and a glulam (glued laminated timber) post-and-beam frame arranged on a 4.8 m grid.

Lateral resistance is provided by the CLT core and full-height perimeter glulam diagonals. Wind-induced occupant comfort was identified early on as the governing design criterion. A two-stage wind-engineering approach was implemented (Laurent et al., 2023): stage (1) Analytical calculations utilized Eurocode-1-4 (Eurocode 1-4, 2010) for along-wind effects, NBCC procedures (NBCC-Guidelines, 2017; NBCC, 2018) for across-wind effects, and additional references (Konrad and Johann-Dietrich, 2003) for torsional response and combination of accelerations. These were assessed against the ISO 10137 (ISO 10137, 2007) comfort limits. A structural damping ratio of 1.9 % was assumed: Parametric studies revealed that the top-floor mass and core-panel connection stiffness were the most influential factors on acceleration (Laurent et al., 2023). Notably, a 20 % variation in connection and bracing stiffness had a negligible effect on acceleration (Laurent et al., 2023). The natural frequencies of the first three modes are: 0.72 Hz and 0.57 Hz for the two translational modes, and 0.97 Hz for the torsional mode (Laurent et al., 2023). Stage (2) A 1:200 scale rigid-model wind tunnel test was performed, taking the surrounding context into account (Laurent et al., 2023). The wind tunnel predicted peak accelerations at the highest occupied level of 0.70 % g for a 1-year return period and a 2.40 % g for a 10-year return period—both results remain within ISO 10137 (ISO 10137, 2007) limits for office use.

This section examines the wind-induced vibration design of five completed high-rise timber buildings, selected for their height rankings and the availability of detailed public information. The review shows that:

- Wind actions already dominate the structural design of most high-rise timber buildings. Because existing towers such as Mjøstårnet have reached—or slightly exceeded—comfort limits (Abrahamsen, 2017), wind consideration will likely continue to govern the design of even taller timber structures.
- Current practice for the design of high-rise timber buildings against wind-induced vibration concentrates on along-wind accelerations, whereas across-wind, torsional, and combined responses are often

neglected. This omission is significant: across-wind accelerations can exceed the along-wind component, and combined responses can surpass any single-direction value. Designs that ignore these additional effects are therefore prone to underestimating wind-induced accelerations, potentially compromising occupant comfort.

- Wind-induced vibrations are mass-dependent. In the design of high-rise timber buildings, adding mass—by incorporating concrete or timber-concrete-composite (TCC) floor slabs, either partially or throughout—can effectively reduce wind-induced vibration responses.
- Three of the five high-rise timber-framed buildings analyzed, incorporated concrete cores to enhance lateral resistance, including the world’s tallest timber building, demonstrating the effectiveness of this approach in improving wind performance. However, efficient lateral load transfer remains critical, necessitating careful design of intercomponent connections to ensure forces are properly transmitted to the core. Future structural optimization and design trends in high-rise timber-framed buildings driven by wind resistance merit continued attention.
- The damping values selected for the timber structures studied range between 1.5 % and 1.9 %, offering useful reference points; However, their applicability and accuracy require further investigation.
- The absence of damping devices in current high-rise timber structures to mitigate wind-induced vibrations highlights an important area for future exploration. Meanwhile, developing efficient, compact dampers tailored to the specific characteristics of high-rise timber buildings remains a significant design challenge.

5. Conclusions and outlook

This paper presents a comprehensive study of design criteria, codes and standards, and built examples related to wind-induced vibration in high-rise timber buildings. The findings offer practical guidance for researchers, design professionals, and regulatory bodies concerned with the wind performance of high-rise timber structures. The study identifies several interrelated shortcomings in the existing criteria, codes, and documented case studies in this field.

In terms of design criteria, the proliferation of largely non-mandatory guidelines complicates their practical application. Each criterion is anchored to wind speeds associated with a specific return period; however, reliable procedures for translating these limits to alternative return periods are generally lacking. Furthermore, most criteria treat wind-induced responses along a single axis in isolation, offering minimal guidance on how to evaluate combined along-wind, across-wind, and torsional effects.

The reviewed codes and standards likewise exhibit notable limitations. Many do not provide complete calculation procedures for all vibration components or limit their applicability to specific cross-sectional shapes and aspect-ratios that do not account for modern tall timber designs. As a result, designers often need to adopt supplementary methods. When procedures do exist, the assumptions for natural-frequency estimation and damping ratios are typically based on reinforced-concrete or steel structures. This situation forces practitioners to look for additional references or perform custom analyses. It highlights an urgent need for timber-specific models to estimate natural frequencies and, especially, empirically calibrated formulas and validated ranges for damping ratios.

An examination of completed projects highlights a predominant focus on along-wind acceleration, while across-wind and torsional responses—as well as their combined effects, are less frequently addressed. Due to their lighter self-weight, timber buildings tend to reach critical acceleration thresholds at relatively modest heights. For example, at Mjøstårnet the predicted along-wind accelerations marginally exceeded comfort limits near the upper levels (around 68.2 m) (Abrahamsen, 2017). These observations suggest that wind performance will likely play a crucial role in the overall design of future high-rise

timber structures. In this case, optimizing the structural systems of high-rise timber buildings for wind resistance will become increasingly critical, and the incorporation of damping devices may prove essential. As a mitigation measure for current design practice, incorporating concrete/TCC floors and a concrete core increases mass and stiffness, thereby reducing wind-induced accelerations.

The findings of this paper underscore the urgent need to establish consistent wind-induced vibration design codes and standards for high-rise timber structures, particularly with clear methods for estimating natural frequencies and well-founded recommendations for selecting damping values. Moreover, further research is essential, especially on predicting and calculating wind-induced effects in timber buildings with multiple-order vibration modes and irregular cross-sections, optimizing structural configurations for wind resistance, developing damping systems tailored to timber high-rises, and conducting long-term vibration monitoring. The limitations of this paper include the lack of an in-depth discussion of the theoretical principles underlying the wind-induced vibration calculation methods provided in various codes, as well as the omission of standards from emerging regions with growing potential for high-rise timber development (e.g., China and India).

CRedit authorship contribution statement

Haoze Chen: Conceptualization, Data curation, Formal analysis, Investigation, Methodology, Resources, Validation, Visualization, Writing – original draft, Writing – review & editing. **Libo Yan:** Conceptualization, Data curation, Formal analysis, Funding acquisition, Investigation, Methodology, Project administration, Resources, Supervision, Validation, Writing – original draft, Writing – review & editing. **Junaïd Ajaz Dand:** Formal analysis, Investigation.

Declaration of competing interest

The authors declare that they have no known competing financial interests or personal relationships that could have appeared to influence the work reported in this paper.

Acknowledgements

This work forms part of the project “Erstellung eines Leitfadens zum Bauen mehrgeschossiger Gebäude mit Holz unter expliziter Berücksichtigung von Windlasten (LeiWind) (Development of a guideline for the construction of multi-storey buildings with wood with explicit consideration of wind loads)”. The authors gratefully acknowledge financial support from the Fachagentur Nachwachsende Rohstoffe e.V. (FNR, Agency for Renewable Resources), funded by the German Ministry of Agriculture, Food and Regional Identity (BMLEH), Grant No. 2221HV069A (Verbundvorhaben) and 2221HV069B (Verbundvorhaben).

Data availability

Data will be made available on request.

References

Abrahamsen, Rune, 2017. Mjøstårnet-construction of an 81 m tall timber building. In: 23. Internationales Holzbau-Forum IHF 2017. Innsbruck, 06.-08.12.2017.

Abrahamsen, R., 2018. Mjøstårnet-18 Storey Timber Building Completed, 24th Internationales Holzbau-Forum (IHF 2018). Garmisch-Partenkirchen, Germany.

agreement, Paris, 2017. Paris agreement. Paris agreement. In: Report of the Conference of the Parties to the United Nations Framework Convention on Climate Change, vol. 2.

AIJ-Guidelines, 1991. Guidelines for the Evaluation of Habitability to Building Vibration. Architectural Institute of Japan, Tokyo.

AIJ-Guidelines, 2004. Guidelines for the Evaluation of Habitability to Building Vibration. Architectural Institute of Japan, Tokyo.

AIJ-RLB, 2004. Recommendations on Loads for Buildings. Part 6 Wind Load. Architectural Institute of Japan, Tokyo.

Alejandro, F., Jordan, K., John, P., 2024. Mass timber hybrid high-rise in Milwaukee sets precedents. <https://www.asce.org/publications-and-news/civil-engineering-source/civil-engineering-magazine/issues/magazine-issue/article/2024/01/mass-timber-hybrid-high-rise-in-milwaukee-sets-precedents>. (Accessed 21 May 2025).

Aloisio, A., Pasca, D.P., Santis, Y. de, Hillberger, T., Giordano, P.F., Rosso, M.M., Tomasi, R., Limongelli, M.P., Bedon, C., 2023. Vibration issues in timber structures: a state-of-the-art review. *J. Build. Eng.* 76, 107098.

Aly, A.M., 2013. Pressure integration technique for predicting wind-induced response in high-rise buildings. *Alex. Eng. J.* 52 (4), 717–731.

ASCE/SEI 7-22, 2022. Minimum Design Loads and Associated Criteria for Buildings and Other Structures. American Society of Civil Engineers. Reston, vol. A.

Ascione, F., Esposito, F., Iovane, G., Faiella, D., Faggiano, B., Mele, E., 2024. Sustainable and efficient structural systems for tall buildings: exploring timber and steel-timber hybrids through a case study. *Buildings* 14 (2), 524.

AS/NZS 1170.0. 2002. Structural Design Actions. Part 0: General Principles. Sydney & Wellington: Standards Australia Ltd & Standards New Zealand.

AS/NZS 1170.2. 2021. Structural Design Actions. Part 2: Wind Actions. Sydney & Wellington. Standards Australia Ltd & Standards New Zealand.

Burton, M.D., Kwok, K.C., Hitchcock, P.A., Denoon, R.O., 2006. Frequency dependence of human response to wind-induced building motion. *J. Struct. Eng.* 132 (2), 296–303.

Canadian Wood Council, 2018. Brock commons tallwood house. UBC VANCOUVER CAMPUS the advent of tall wood structures in Canada A CASE STUDY. https://cwc.ca/wp-content/uploads/2018/04/CS-BrockCommon.Study_.8.pdf.

CNR-DT 207/2008, 2010. Guide for the Assessment of Wind Actions and Effects on Structures. NATIONAL RESEARCH COUNCIL OF ITALY, Rome.

Council on Tall Buildings and Urban Habitat, 2022. Tallest mass timber buildings. <http://www.ctbuh.org/mass-timber-buildings>, 21 May 2025.

Davenport, A.G., 1962. The response of slender, line-like structures to a gusty wind. *Proc. Inst. Civ. Eng.* 23 (3), 389–408.

Duan, Z., Huang, Q., Zhang, Q., 2022. Life cycle assessment of mass timber construction: a review. *Build. Environ.* 221, 109320.

EN 1995-1-1:2005/A2:2014, 2014. Eurocode 5: Design of Timber Structures. Part 1-1: General - Common Rules and Rules for Buildings 91, 010.30 91.010.30. European Committee for Standardization, Brussels.

Eurocode 1-4, 2010. Eurocode 1: Actions on Structures. Part 1-4: General Actions - Wind Actions. EUROPEAN COMMITTEE FOR STANDARDIZATION.

Eurocode 1-4, 2024. Eurocode 1 - Actions on Structures. Part 1-4: Wind Actions. European Committee for Standardization, Brussels.

Feng, R., Yan, G., Ge, J., 2012. Effects of high modes on the wind-induced response of super high-rise buildings. *Earthq. Eng. Vib.* 11 (3), 427–434.

Fernandez, A., Komp, J., Peronto, J., 2020. Ascent-challenges and advances of tall mass timber construction. *International Journal of High-Rise Buildings* 9 (3), 235–244.

Gheuens, J., 2024. The European green deal. In *making the European green deal work. EU sustainability policies at home and abroad*. In: Dyrhaage, H., Kurze, K. (Eds.), *Routledge Studies on the Governance of Sustainability in Europe*. Routledge, Abingdon Oxon, New York NY, pp. 15–28. <https://doi.org/10.4324/9781003246985-3>.

GoTo, T., 1983. Studies on wind-induced motion of tall buildings based on occupants' reactions. *J. Wind Eng. Ind. Aerod.* 13 (1–3), 241–252.

Hansen, C.H., 2007. Effects of low-frequency Noise and Vibration on People. Multi-Science Pub. Co, Brentwood Essex.

Hansen, R.J., Reed, J.W., Vanmarcke, E.H., 1973. Human response to wind-induced motion of buildings. *ASCE Journal of Structural Division* 99 (7), 1589–1605.

Howarth, H., 2015. Human exposure to wind-induced motion in tall buildings: and assessment of guidance in ISO 6897 and ISO 10137. In: 50th UK Conference on Human Responses to Vibration, vol. 267, 9-10 September 2015, Southampton, United Kingdom.

IBC, 2024. International Building Code. International Code Council (ICC).

ISO 10137, 2007. Bases for Design of Structures. Serviceability of Buildings and Walkways. International Organization for Standardization, Geneva.

ISO 6897, 1984. Guidelines for the Evaluation of the Response of Occupants of Fixed Structures, Especially Buildings and off-shore Structures, to low-frequency Horizontal Motion (0,063 to 1 Hz). International Organization for Standardization, Geneva.

Konrad, B., Johann-Dietrich, W., 2003. Beton-Kalender 2003: Hochhäuser Und Geschossbauten. Ernst & Sohn, Berlin.

Kwon, D.K., Kareem, A., 2013. Comparative study of major international wind codes and standards for wind effects on tall buildings. *Eng. Struct.* 51, 23–35.

Lamb, S., Kwok, K., Walton, D., 2013. Occupant comfort in wind-excited tall buildings: motion sickness, compensatory behaviours and complaint. *J. Wind Eng. Ind. Aerod.* 119, 1–12.

Laurent, G., Anthony, R., Guillaume, C., Tim, S., Lucia, T., Johannes, P., Tobias, W., 2023. Design of a tall mass timber tower for occupant comfort under wind-induced accelerations. In: World Conference on Timber Engineering Oslo 2023, pp. 4316–4324.

Live, H., Abrahamsen, R., 2023. Mjøstårnet: the WORLD'S tallest timber building. World Conference on Timber Engineering 2023 1, 19–22.

Michele, M., Daniel, P., Rob, V., Jamie, D., Pavel, T., 2023. Dynamic performance of hybrid timber-concrete high-rise under wind induced excitation measured through On-Site testing. SECED 2023 Conference Earthquake Engineering & Dynamics for a Sustainable Future, pp. 14–15. Sep. 2023, Cambridge, UK.

Nathan, Benbow, 2019. 55 southbank boulevard Melbourne challenges of a 10-Storey mass timber vertical extension. Proceedings of the 25th Internationales Holzbau-Forum (IHF 2019) 3, 121–126.

- National annex to NEN-EN 1990+ A1+A1/C2: eurocode: basis of structural design, Technische Grondslagen Voor Bouwconstructies. Normcommissie 351 001, 2011.
- NBCC, 2018. National Building Code of Canada 2015. National Research Council of Canada, Ottawa.
- NBCC-Guidelines, 2017. User's Guide - NBC 2015: Part 4 of Division B (Structural Commentaries). National Research Council of Canada, Ottawa.
- Poirier, E., Moudgil, M., Fallahi, A., Staub-French, S., Tannert, T., 2016. Design and construction of a 53-meter-tall timber building at the university of British Columbia. In: Proceedings of the World Conference on Timber Engineering, Vienna, Austria.
- Porteron, Samy, 2023. Seeing the Forest Through the Trees: How Sustainable Timber Buildings can Help Fight the Climate Crisis. ECOS. <https://ecostandard.org/wp-content/uploads/2023/02/ECOS-REPORT-How-sustainable-timber-buildings-can-help-fight-the-climate-crisis-March-2023.pdf>.
- Skullestad, J.L., Bohne, R.A., Lohne, J., 2016. High-rise timber buildings as a climate change mitigation measure – a comparative LCA of structural system alternatives. Energy Proc. 96, 112–123.
- Svatoš-Ražnjević, H., Orozco, L., Menges, A., 2022. Advanced timber construction industry: a review of 350 multi-storey timber projects from 2000–2021. Buildings 12 (4), 404.
- Tamura, Y., 2003. Wind Resistant Design of Tall Buildings in Japan. the 11th International Conference on Wind Engineering, Lubbock, Texas.
- Tulebekova, S., Ao, W.K., Pavic, A., Malo, K.A., Rønquist, A., 2024. Identification of modal properties of a tall glue-laminated timber frame building under long-term ambient vibrations and forced vibrations. ASEC Journal of Structural Engineering 150 (10), 4024125.
- Tulebekova, S., Malo, K.A., Rønquist, A., Nævik, P., 2022. Modeling stiffness of connections and non-structural elements for dynamic response of taller glulam timber frame buildings. Eng. Struct. 261, 114209.
- Verbundvorhaben, F.N.R.. *Erstellung eines Leitfadens zum Bauen mehrgeschossiger Gebäude mit Holz unter expliziter Berücksichtigung von Windlasten; Teilvorhaben 1: projektkoordination, experimentelle und numerische Untersuchungen zum Schwingungsverhalten* - Akronym: LeiWind. <https://baustoffe.fnr.de/index.php?id=11492&fkz=2221HV069A>.
- Verbundvorhaben, F.N.R.. *Erstellung eines Leitfadens zum Bauen mehrgeschossiger Gebäude mit Holz unter expliziter Berücksichtigung von Windlasten; Teilvorhaben 2: schwingungsanalyse und -extrapolation* - akronym: LeiWind. <https://baustoffe.fnr.de/index.php?id=11492&fkz=2221HV069B>.
- Verhaegh, R., Vola, M., Jong, J.de., 2020. Haut. a 21-storey tall timber residential building. International Journal of High-Rise Buildings 9 (3), 213–220.
- Wijesooriya, K., Mohotti, D., Lee, C.K., Mendis, P., 2023. A technical review of computational fluid dynamics (CFD) applications on wind design of tall buildings and structures: past, present and future. J. Build. Eng. 74, 106828.
- World Green Building Council, 2019. Bringing Embodied Carbon Upfront. Coordinated Action for the Building and Construction Sector to Tackle Embodied Carbon. World Green Building Council. <https://worldgbc.org/article/bringing-embodied-carbon-upfront/>.
- Woschitz, Richard, 2015. Holzhochhaus HoHo Wien. the technical solution. In: 21st Internationales Holzbau-Forum IHF, Garmisch-Partenkirchen, vols. 2–4.
- Yan, L., Klingner, R., Al-Qudsi, A., Chen, H., Dand, J.A., 2025. Current market landscape and industry voices in key timber construction markets. Buildings 15 (18), 3381.